10-27-2008

Investigation and Evaluation of a Bi-Polar Membrane Based Seawater Concentration Cell and Its Suitability as a Low Power Energy Source for Energy Harvesting/MEMS Devices

Clifford Ronald Merz
University of South Florida, cmerz@usf.edu

Investigation and Evaluation of a Bi-Polar Membrane Based Seawater Concentration Cell and Its Suitability as a Low Power Energy Source for Energy Harvesting/MEMS Devices

by

Clifford Ronald Merz

A dissertation submitted in partial fulfillment
of the requirements for the degree of
Doctor of Philosophy
Department of Electrical Engineering
College of Engineering
University of South Florida

Major Professor: Wilfrido A. Moreno, Ph.D.
Marilyn Barger, Ph.D.
Kenneth A. Buckle, Ph.D.
Stephen M. Lipka, Ph.D.
Paris H. Wiley, Ph.D.

Date of Approval:
October 27, 2008

Keywords: Dialytic Battery, Fuel cell, Semi-permeable membrane, Renewable energy, Ocean energy, Anomalous Osmosis, Salinity Gradients, Electrochemical testing

Acknowledgements

I would like to express a heart felt thanks to my major-professor Dr. Wilfrido Moreno and all my committee members for their continual support and participation during this long adventure. I'm also indebted to Professors Luis García-Rubio, College of Marine Science, and Alberto A. Sagüés, Department of Civil and Environmental Engineering, for their guidance, encouragement, and generous use of lab space and equipment. Many thanks, as well, to Dr. Robert Carnahan, USF Professor Emeritus, whose exposure to Desalination Science both ignited and fueled my interest in this exciting technology and for whose unselfish dedication early on in my program made such a difference in this becoming a reality. Many thanks to: Mr. Tony Greco, USF College of Marine Science, for the SEM/X-Ray imagining; to Kingsley Lau, USF Civil and Environmental Engineering Ph.D. Candidate, whose help and friendship will always be appreciated; and to Vembu Subramanian, USF College of Marine Science, whose friendship and supportive greetings of "Dr. Cliff" during this journey were always appreciated. To my wife and family, whose sacrifices were many as I pursued this full time obsession on a part time basis. And finally, to my parents, especially my Dad, for without his lifelong encouragement, and steadfast support, none of this would have happened.

Table of Contents

List of Tables

List of Figures

Investigation and Evaluation Of A Bi-Polar Membrane Based Seawater Concentration Cell and Its Suitability as a Low Power Energy Source for Energy Harvesting/MEMS Devices

Clifford Ronald Merz

ABSTRACT

It has long been known from Thermodynamics and written in technical literature that, in principal, instant energy can be made available when dilute and concentrated solutions are mixed. For example, a river flowing into the sea carries with it a physical-chemical potential energy in its low salt content, some of which should be recoverable. As also known, a naturally occurring, diffusion-driven, spontaneous transport of ions occurs throughout a solution matrix, thru barrier interfaces, or thru ion-selective membranes from the side containing the salts of higher concentration to the compartments containing the more dilute solution to effect the equalization of concentration of the ionic species. Since this ion movement consists, preferentially, of either cations or anions, it leads to a charge separation and potential difference across the membrane, otherwise known as a membrane potential. Eventually, when the concentrations in the compartment are the same, the cell ceases to function. However, if operated as a fuel cell with its respective concentrations continually replenished, equilibrium at a specific value of potential difference is established.

To capture the energy of this potentially significant albeit low power energy source, a suitable energy extraction device is required. The focus of this Ph.D. research effort is to address the concept, research and evaluation of a Bi-Polar membrane based seawater concentration cell and its suitability as a low power energy source for Energy Harvesting/MEMS devices (patent pending).

Chapter 1

Introduction

1.1 Focus and Direction

A concentration cell is an electrochemical cell consisting of a semi-permeable ion-exchange membrane between two solutions containing the same electrolyte in different concentration. With no external voltage applied, a naturally occurring, diffusion-driven (osmotic), spontaneous transport of ions occurs through the ion-exchange membrane. Ion-exchange membranes between solutions act as a barrier across which almost no electrolyte can diffuse. Theoretically, the free energy of the system can be completely converted into electric energy.

Since ion movement consists, preferentially, of either cations or anions, it leads to a charge separation known as a potential difference across the membrane. Non-replenishing concentration cells using single anion/cation ion conducting semi-permeable membranes have been examined in the past, however, the idea of a replenishing Bi-Polar membrane based concentration cell for instant energy generation is unique and innovative, and is the basis of this research dissertation.

This renewable instant energy has uses in a wide variety of applications and size scales depending upon the source of the supplied ionic solutions and the anticipated scale/end use of the system. Some of these applications include, but are not limited to: Micro/Nano capacity direct power generation systems required for energy harvesting and nanotechnology low power devices; low power electronic, communication devices (e.g., Pico-Radio, or SCADA); devices operated in the marine environment; Medium scale supplemental power generation (such as direct and energy recovery devices used in power generation and desalination plants); Large scale direct commercial power generation systems using naturally occurring salinity gradient differences such as those found where rivers discharge into the sea; and as a possible supplemental energy source for use in the generation of H^+ (protons) via membrane water dissociation (or splitting) technology.

One envisioned use, and the focus of this dissertation effort, is to provide energy to low power remote sensor networks or wireless monitoring technologies where it is impractical or impossible to provide wired power. Successful application will result in a combined energy harvester/generator and storage system capable of providing the very small amounts of power required to couple with and take advantage of miniaturized, low-power electronics, wireless standards, and modern technologies such as Micro-ElectroMechanical Systems (MEMS) fabricated using standardized semiconductor processing techniques.

1.2 Motivation and Purpose

The overarching contribution and technical objective of this Ph.D. research is to develop increased technical understanding into the ionic, environmental, and electrochemical effects on the generated current and voltage of a membrane based seawater concentration cell. Knowledge obtained from this effort will lead to the development of innovative engineering process schemes, designs, and equipment for economic generation, based on the applied concepts of recovery and reuse of energy released from salinity concentration gradient differences: for both defense and domestic applications.

Utilizing modern standardized semiconductor processing techniques, it is possible to make very small, inexpensive sensors. It is desirable, if not necessary, to provide small, low power systems for these devices. Therefore, considering the near limitless source of ionic solutions, the market and technological impact is enormous. Potential impact of the increased technical understanding derived from this research effort can be practically and immediately applied to the development of such a suitable low power system. The intent of this research effort is to:

1) Develop increased technical understanding into the membrane, ionic, environmental, and electrochemical effects because of charge separation effects of a Bi-Polar semi-permeable membrane based, seawater concentration cell (patent pending),

2) Examine the feasibility/applicability of this Dialytic based membrane concentration cell as a power source for energy harvesting devices (patent pending),

3) Evaluate possible MEMS based applications (patent pending).

1.3 Participants

Dialytics, Inc. (Dialytics) is a small business technology spin-off entity founded by Clifford R. Merz to undertake development of a University of South Florida (USF) technology he invented and was the focus of this research effort. Dialytics and USF's Division of Patents and Licensing have entered into a technology license agreement for development and ultimate commercialization of this technology. As such, Dialytics is the research sponsor and technology licensee while Mr. Merz is the project principal investigator.

Chapter 2

Required Technical Background and Discussion

2.1 Summary of Rule Basics with respect to Cell Reactions and EMF[1]

A fuel cell is an electrochemical system which converts the free energy change of an electrochemical reaction into electrical energy. In dealing with the energy relations of cells, thermodynamic principles find very extensive applications. However, the use of these principles is subject to one very important restriction, namely, that the processes to which the principles are applied are reversible. It is recalled that the conditions for thermodynamic reversibility of processes are (a) that the driving and opposing forces be only infinitesimally different from each other and (b) that it should be possible to reverse any change taking place by applying a force infinitesimally greater than the one acting.

The net electrical work performed by a reaction yielding an electromotive force (EMF) and supplying a quantity of electricity (q) is qE. The EMF of a battery (or other source) is the maximum potential difference (E). But that can be reduced by the drop across the internal resistance of the source. In the real world, there is always an internal resistance, and in batteries the internal resistance increases with time and usage. So the potential difference is the actual measured voltage while EMF is what you would

measure in a resistance-free device. Each equivalent reacting q is equal to the faraday F, hence for n equivalents reacting, q = nF. The electrical work obtained from any reaction supplying nF coulombs of electricity at a potential E° is:

$$\text{Net electrical work} = nFE^{\circ}$$

But any work performed by a cell can be accomplished only at the expense of a decrease in free energy. Further, when the electrical work is a maximum, as when the cell operates reversibly, the decrease in free energy, $-\Delta G$, must equal the electrical work done as presented in Equation 1,

$$\Delta G = -nFE^{\circ} \qquad \textit{Equation 1}$$

E° is the reversible potential and is derived from the free energy change for the reaction. The reversible EMF of any cell is determined by the free energy change of the cell and Equation 1 is the "bridge" between thermodynamics and electrochemistry. Information provided by EMF measurements assist in the evaluation of thermodynamic properties.

For any spontaneous reaction at constant pressure and temperature ΔG is negative, for any nonspontaneous reaction at constant pressure and temperature ΔG is positive, while for any reaction in equilibrium $\Delta G = 0$. In view of this, it may be deduced that for any spontaneous reaction E° will have to be positive, for any nonspontaneous

reaction E° will have to be negative, while for any reaction in equilibrium E° will have to be equal to 0. Summarized in Table 2.1 as follows:

Table 2.1 Relation between Signs of ΔG and E°

Reaction	ΔG	E°
Spontaneous	-	+
Nonspontaneous	+	-
Equilibrium	0	0

2.2 Electrochemical Cells – Types and Definitions[2]

Electrochemical cells in which Faradaic currents are flowing are classified as either *galvanic* or *electrolytic* cells. A *galvanic* cell is one in which reactions occur spontaneously at the electrodes when they are connected externally by a conductor (Figure 2.1a). These cells are often employed in converting chemical energy into electrical energy. Galvanic cells of commercial importance include primary (nonrechargable) cells, secondary (rechargeable) cells, and fuel cells. An *electrolytic* cell is one in which reactions are effected by the imposition of an external voltage greater than the open circuit voltage (OCV) of the cell (Figure 2.1b). These cells are frequently used to carry out desired chemical reactions by expending electrical energy. Commercial processes involving electrolytic cells include electrolytic syntheses (e.g., the production

of chlorine), electrorefining (e.g., copper) and electroplating (e.g., silver and gold). The lead-acid storage cell, when being "recharged", is an electrolytic cell.

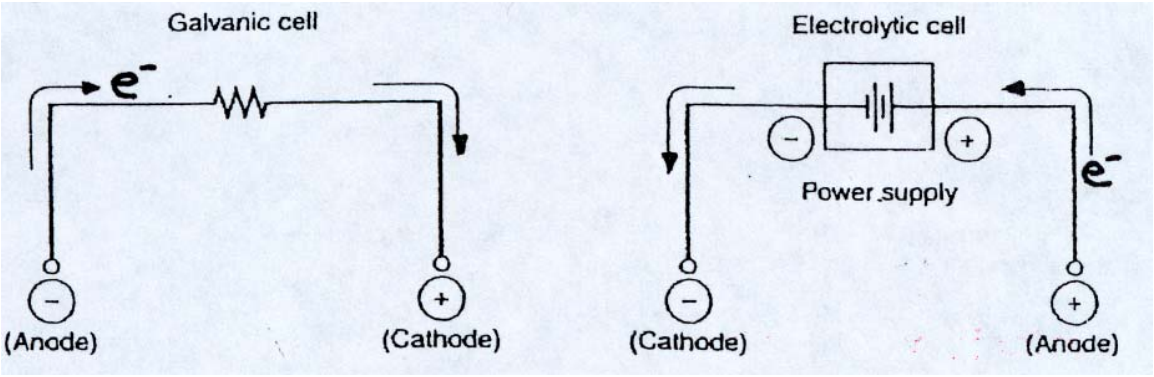

Figure 2.1 Galvanic (a) and Electrolytic (b) Electrochemical Cells

In discussing Electrochemical cells, the following rules are generally used:

1) Cell reaction is the sum of the single electrode reactions as they occur in the cell.
    a) The half-cell, called the anode (positive electrode**),** reaction is oxidation (looses electrons - becomes more negative) – Attracts anions.
    b) The half-cell, called the cathode (negative electrode**),** reaction is reduction (gains electrons – gets less negative or more positive) – Attracts cations.
2) The total cell EMF is the algebraic sum of the single electrode potentials provided each EMF be affixed with the sign corresponding to the reaction as it actually takes place at the electrode.
3) A current in which electrons (e^-) cross the interface from the electrode to a species in solution is a cathodic current, while electron flow from a solution species into the electrode is an anodic current.

4) In an electrolytic cell, the cathode is negative with respect to the anode; but in a galvanic cell, the cathode is positive with respect to the anode.

2.3 Dialytic Power Generation

Because concentration gradient driven systems force ion migration from the high concentration side to the low, they are sometimes referred to as Reverse Electrodialysis or Dialytic systems. Dialytic Power Generation Systems can be operated as a fuel cell (an electrochemical cell in which the chemical energy in a fuel is converted directly into electrical energy) or a battery depending upon if the source of the energy is continually fed to the cell or internally stored and consumed[3] (patent pending). The relationship between the membrane OCV potential and the standard-state Gibbs free energy can be calculated by the Nernst equation – A thermodynamically derived equation relating the potential of an electrochemical cell to the concentration of products and reactants. The applicability of the Nernst equation for a concentration cell under external electrical loading will be determined during this research effort.

2.4 Concentration Cell Basics

A concentration cell is an electrochemical cell consisting of a porous divider between two solutions containing the same electrolyte in different concentrations. With no external voltage applied, a naturally occurring, diffusion-driven (osmotic), spontaneous transport of ions occurs across the separating barrier, in this case a semi-

permeable ion-exchange membrane, across which almost no electrolyte can diffuse. Theoretically, the free energy of the system can be completely converted into electric energy. Since ion movement consists, preferentially, of either cations or anions, it leads to a charge separation across the membrane called a membrane potential. Using reversible electrodes of identical composition inserted into the two identical solutions of differing concentrations, the potential difference can be measured directly.

2.4.1 Concentration Cells with Transference[1]

Unlike chemical cells where in EMF arises from a chemical reaction, concentration cells depend for their EMF on a transfer of material from one electrode to another due to a concentration difference between the two. For example, for a concentration cell containing electrodes made up of the same materials (e.g., Silver [Ag]), solutions containing the same ions but at different concentrations where $C_{conc} > C_{Interface} > C_{dilute}$, and a semi-permeable junction separating the two, the electrical current transferring across the membrane can be analyzed using the following expression:

$$\text{Ag(s)} \mid \text{Seawater (conc)} \;||_{AEM}\; \text{NaCl aq. Soln (Interface)} \;||_{CEM}\; \text{Seawater (dilute)} \mid \text{Ag(s)}$$

Since the same electrode is used in each side of the cell, the EMF of the Galvanic Cell $E_{cell} = E^{o}_{Cathode} - E^{o}_{Anode} = 0.00$ VDC.

This is a dilution process, sodium cations permeate through the Cation Exchange Membrane (CEM) from right to left and chloride ions permeate through the Anion Exchange Membrane (AEM) from left to right; with the anode compartment becoming more concentrated and the cathode compartment more dilute. Through a suitable electrode system, the chemical potential becomes electrical potential.

The OCV membrane potential of a Bi-Polar membrane is based on an extension of the Nernst equations of monopolar charged semi-permeable membranes to the case of the CEM in series with an AEM and the diffusion boundary layers adjacent to the Bi-Polar membrane. Ionic transport in homogeneously charged membranes such as Bi-Polar ones, which consist of a layered structure of two oppositely charged layers, has received attention because these membranes show several interesting phenomena: specifically permselectivity for mono-valent ions and water splitting[4].

2.5 General Ion-Exchange Membrane Discussion

The heart of any electro-membrane process is the semi-permeable ion-exchange membrane. The main properties required of ion-exchange membranes for success in technical processes are[5]:

1) Low electrical resistance. The permeability for the counter-ions under an electrical potential gradient should be high to minimize the membrane IR drop loss.

2) High permselectivity. It should be highly permeable for counter-ions, but should be impermeable to co-ions, and to non-ionized molecules and solvents.
3) Good mechanical stability. It should be mechanically strong, to prevent high degrees of swelling or shrinking due to osmotic effects, when transferred from concentrated to diluted salt solutions and vice versa, and be dimensionally stable.
4) Good chemical stability. It should be stable over a wide pH-range and in the presence of oxidizing agents.
5) Good operating characteristics. Operation over a wide range of current densities and under varying conditions of temperature, current density, pH, pressure, etc.
6) Good water permeability.

The stability of a membrane is of paramount importance because of their high cost, membranes are required to operate for periods of several years. A factor in the operation of cells with membrane is the transport of solvent (e.g., water) which accompanies the transferring ions. In aqueous systems, the transport of water can be significant (e.g., 3-5 water molecules accompany one sodium ion in a chlorine cell). If protons (hydrogen ions) are transferred then typically, two molecules of water are transferred per ion.

2.5.1 Ion-Exchange Membranes[6]

The most important feature, which distinguishes ion-exchange from isotopic-exchange membranes, is the electric coupling of the ionic fluxes. Conservation of

electroneutrality requires stoichiometric exchange, i.e., the fluxes (in equivalents) of the exchanging counter ions must be equal in magnitude; otherwise, a net transfer of electric charge would result. The regulating mechanism that enforces the equality of the fluxes is the electric field (diffusion potential) set up by the diffusion process that produces an electric transference of both counter ions in the direction of diffusion of the slower counter ion; this electric transference is superimposed on the diffusion. The resulting net fluxes of the counter ions are equivalent to one another, while purely diffusional fluxes, as a rule, are not. Thus, electroneutrality is preserved.

If an ionic electro-membrane is in contact with an ionic solution, a distribution of ions in the solution will be established as well as a distribution inside the membrane (Donnan equilibrium). If the membrane has a negative fixed charge, ions of opposite charge (positively charged ions or counter-ions) will be attracted towards the membrane surface while ions of the same charge (negatively charged ions or co-ions) are repelled from the membrane surface. Ions with the same charge as the fixed ions (co-ions) are excluded and cannot pass through the membrane. This effect is known as the Donnan exclusion. Because of the fixed charge, there will be an excess of counter ion charge at the interface and a so-called electrical double layer (EDL) is formed. Protons and Hydroxyl ions are not effectively retained by a Donnan potential and this allows removing these ions from other ions with the same charge. In a basic solution (pH > 7), an ideal CEM is able to retain all anions except for hydroxyl ions. Similarly, an ideal AEM retains all cations except for protons and a separation can be achieved between protons and other cations.

Electric current in an ion-exchange membrane transfers predominantly via counter-ions by diffusion. The simple Nernst equation holds reasonably well within the concentration range of about 10^{-4} to 10^{-1} N. Deviations at higher solution concentrations are caused by co-ion transference, and at lower concentrations by H^+ or OH^- (hydroxyl) ions (stemming from dissociation of H_20) that compete with the electrolyte counter ion (*i.e.,* the increasing concentration of the co-ion in the ion exchanger causes a decrease in the transport number of the counter-ion).

Using the Nernst equation, the maximum reversible OCV (E_{rev}) generated across the membrane of a concentration cell using an ideal permselective membrane as a salt bridge, a 1,1 valence electrolyte, and carefully selected electrodes of identical composition in both compartments can be calculated using Equation 2 as:

$$E_{rev} = E_{cell} - (RT/nF) \ln (a_{\pm} \text{ conc}/a_{\pm} \text{ dil})^{\nu} \qquad \textit{Equation 2}$$

where $a_{\pm}$ = ionic activities (approx. concentrations), n is the number of electrons transferred, and ν = charge on the active ion. Considering an ideal membrane (a = 1.0), monovalent active ion, and a 1:10 activity ratio for the two solutions (i.e., concentrated solution = 10*dilute) the OCV obtained is:

$$E_{rev} = 0.0 - [\nu*(8.314 \text{ J K}^{-1} \text{ mol}^{-1} * 298\text{K}) / 1*96{,}500 \text{ C mol}^{-1}] \ln (0.1)$$

$$E_{rev} = +0.059 \text{ V (spontaneous)}$$

Note that because the same electrode is used in the cell, E_{cell} is zero in the Nernst Equation (see Section 2.4.1). The membrane potential may be higher if the co-ion is more mobile than the counter-ion and if there is little Donnan exclusion of the co-ion**.**

2.5.2 Characterization of Ionic Membranes[7]

Polyelectrolytes are a special class of polymers that contain charged ionic groups, with the properties completely determined by the presence of the ionic groups. Besides the fixed charge present, the properties of solubility, diffusivity, and pore size distribution affect separation. Charged membranes or ion-exchange membranes are typically employed in electrically driven processes such as Electrodialysis (ED) and membrane electrolysis as well as pressure or concentration driven processes such as diffusion dialysis and Donnan dialysis (combination of Donnan exclusion and diffusion).

Strong attractions exist between counter ions and the membrane fixed charge groups. As mentioned, Polylelectrolytes that contain a fixed negatively charged group fixed to the polymeric chain are called Cation Exchange Membranes (CEM) because they are capable of exchanging positively charged cations. When the fixed charged group is positive, the polyelectrolytic membrane is called an Anion Exchange Membrane (AEM) because it is capable of exchanging negatively charged ions. The counter ions (ions with charge opposite to the fixed charge group), can move freely within the limits of the Coulomb forces and electroneutrality. A schematic representation of typical membranes of both types is given in Figure 2.2.

Cation Exchange Membrane (CEM)

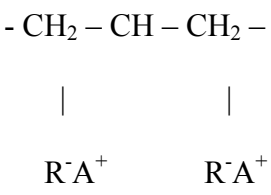

Where R = - $SO3^-$ (Sulfonic Acid Group)

- COO^- (Carboxylic Acid Group)

Anion Exchange Membrane (AEM)

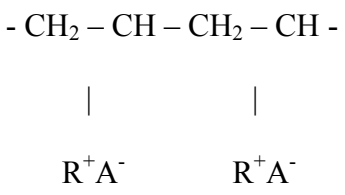

R = $N(CH)_3^+$ (Quaternary Ammonium Salt Group)

Figure 2.2 Schematic Representations of Typical Ion-Exchange Membranes

In water or other strongly polar solvents polyelectrolytes are ionized. However, unless cross-linked, the polymer potion will swell or even become soluble because of its high affinity to water. Even very hydrophobic polymers such as polysulfone can be made water-soluble by introducing a large number of sulfonic groups. A very interesting polymer for preparing ionic membranes is Polytetrafluororethylene. This polymer is very stable with respect to chemicals, pH and temperature. Ionic groups can be introduced into this polymer to yield a very stable polyelectrolyte based on a Teflon matrix. One such polymer obtained on this basis is Nafion® shown in Figure 2.3 below.

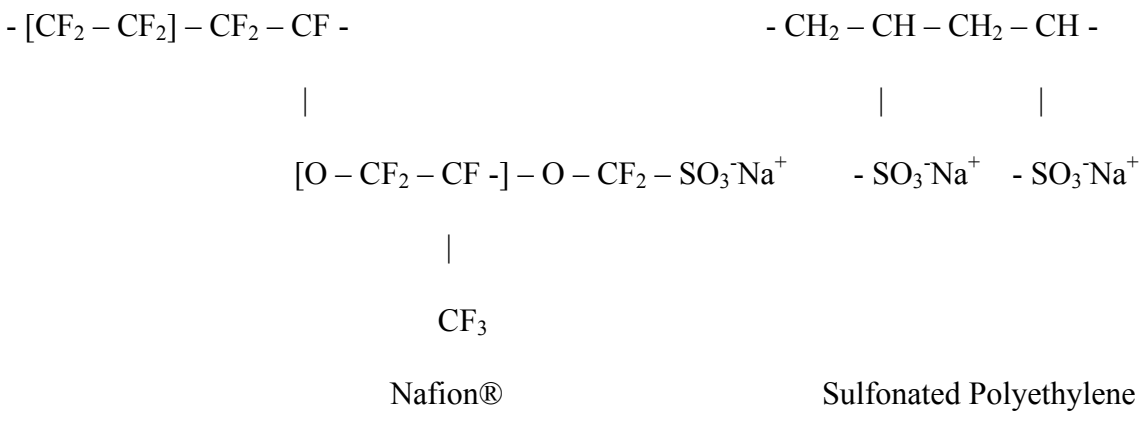

Figure 2.3 Chemical Structures for Nafion® and Sulfonated Polyethylene CEM

Cation selective membranes are usually made of cross-linked poly (styrene-co-divinylbenzene) base polymer that has been sulfonated to produce sulfonate groups [$-SO_3^-$] or carboxylate groups [$-COO^-$] attached to the polymer. Anion membranes can be cross-linked poly (sulfone) base polymer containing quaternary ammonium groups [$-N(CH)_3^+$]. Currently, aliphatic anion membranes are favored because they have lower electrical resistance[8].

Homogeneous membranes are coherent, unsupported gels. Heterogeneous membranes are prepared by incorporating colloidal ion-exchanger particles into an inert binder. To obtain structural support, a membrane is fabricated by applying the cation- and anion-selective polymer to a fabric or wide-mesh plastic tissues material[9]. Membranes are made in flat sheets and contain about 30 to 50% water. Each membrane has a network of molecular-size pores that are too small to allow significant water flow and that have electronegative [$-SO_3^-$] or electropositive [$-N(CH)_3^+$] fixed charges[10].

For electrical neutrality to be maintained, each of the fixed charges on the membrane must be associated with an ion of the opposite charge. The ion can easily move from one fixed charge to another. Thus, the membrane can pass an electrical current in the form of migrating ions. Since the fixed-charged groups on the membrane repel like-charged ions, anions cannot enter the anion selective membrane[11]. Not being perfectively semi permeable, the membranes do not completely reject ions of the same charge. However, their permselectivity is > 90%.

2.5.3 Diffusion in Ion-Exchange Membranes

When sodium chloride (NaCl) is dissolved in water, it is ionized and dissociates into hydrated Na^+ (aq) cations and Cl^- (aq) anions. Strong electrolytes, such as Na^+ (aq) and Cl^- (aq), are so well hydrated that they are too far apart to interact directly with each other, even in solutions of great ionic strength. Ions that are so well hydrated that they experience only nonspecific interactions with each other are termed “free ions”. Ions not so well hydrated can come into closer contact. In cases where ions are close enough to share some of their primary salvation shells, the resulting strong electrostatic attraction is referred to as ion pairing[12].

Because ions are hydrated in solution and the extent of hydration depends on the charge and size of the ion, di-and tri-valent ions move more slowly across the membrane than do monovalent ions. Accordingly anions such as Cl^- pass through the electro-membranes more readily than H^+, Na^+, K^+, and other cations. Sodium chloride in water

does not diffuse as a single molecule; instead the sodium ions and chloride ions move freely through the solution. Although the sodium ion diffuses more slowly than the chloride ion, the diffusion of sodium chloride can be accurately described by a single average diffusion coefficient. Protons and hydroxyl ions have unusually high diffusion constants.

The ion-exchange mechanism is primarily a redistribution of the counter ions by diffusion. The co-ion has relatively little effect on the kinetics and the rate of ion exchange. The basic equation used to compare various membrane processes when transport occurs by diffusion is given in Equation 3 as:

$$J_i = (\beta_i/d)*(c_{i,1}^{s} - \alpha_i\, c_{i,2}^{s}\ \exp\,[-V_i\,(P_1-P_2)/RT]) \qquad \textit{Equation 3}$$

Where, J_i = Flux of component I through the membrane; m/s

V_i = Molar Volume (m^3/mol)

β_i = Permeability coefficient = D_i (Diffusional Coefficient) * K_i (solubility constant defined as the ratio of activity coefficients)

α_i = $K_{I,2} / K_{I,1}$

d = Membrane thickness (m)

P_1-P_2 = Pressure difference across the membrane (N/m^2)

R = Universal Gas Constant = (J/mole.K)

T = Temperature in Degrees Kelvin (ºC + 273)

In concentration cells, liquid phases containing the same solvent are present on both sides of the membrane in the absence of a pressure difference. The pressure terms can therefore be neglected and Equation 4 developed with the condition of $\alpha_i = 1$ as:

$$J_i = (\beta_i/d)*(c_{i,1}^{s} - \alpha_i\, c_{i,2}^{s}) \qquad \textit{Equation 4}$$

Equation 4 shows that the concentration cell solute flux is proportional to the concentration difference (as in Reverse Osmosis). Separation arises from differences in permeability coefficients: these macromolecules have much lower diffusion coefficients and distribution coefficients than low molecular weight compounds such as salts.

2.6 Bi-Polar Ion-Exchange Membranes and Their Uses

A Bi-Polar membrane consists of a monopolar CEM and monopolar AEM joined together with an intermediate transitional phase layer between. To explain the transport of ions through a charged membrane, the interaction between ions and fixed charge groups inside the membrane as well as at the interface has to be considered. In Bi-Polar membranes, there are 3 interfaces: (i) the interface between the concentrated saline solution and the anion-exchange membrane, (ii) the interface between the anion-exchange membrane and the cation-exchange membrane (intermediate transitional phase layer), and (iii) the interface between the cation-exchange membrane and the dilute saline solution. Among these three interfaces, the intermediate transitional phase layer is the most difficult to observe and the concentration cannot be measured experimentally.

The transport properties of Bi-Polar membranes are quite different from those of monopolar membranes. When an electric field is established across a Bi-Polar membrane the anions and cations contained in the intermediate layer migrate through the AEM and CEM in the direction of the electric field. Because of the current flow the intermediate layer becomes impoverished in salt and its resistance increases. Two EDL and Donnan potential differences develop between the intermediate layer and the outside and are opposite to the applied field.

For a constant outer potential difference, the current density of initial value i_o reduces to a much smaller value i_t with the current density below a limiting current i_{lim}[13]. In the Bi-Polar membrane's matrix the concentration of the counter-ions is equal to the sum of the concentration of the fixed ions and co-ions. As one approaches the intermediate layer of the Bi-Polar membrane the concentration of the mobile ions (counter- and co-ions) decreases until a depleted layer arises in which the mobile ions have a fundamentally lower concentration than the fixed ions.

Although made up of well-defined individual components, once combined the Bi-Polar membrane acquires unique capabilities and additional uses. These include: 1) a variation in membrane potential depending upon which side is in contact with the concentrated solution, which is not the case in monopolar ion-exchange membranes[14], and 2) its use in converting water-soluble salts to their corresponding acids and bases via the process of water dissociation, known also as splitting.

2.6.1 Bi-Polar Membrane Side Orientation

The two-monopolar layers of a Bi-Polar membrane always differ in their fixed ion molarities and in the sign of their charge. These differences are the cause of the asymmetrical character of Bi-Polar membranes[13]. Unlike monopolar ion-exchange membranes[6], in Bi-Polar membranes, the membrane facing direction and the intermediate phase condition will alter the direction of the membrane potential charge. The intermediate layer in a Bi-Polar membrane seems to act as an alteration barrier for the membrane potential according to the membrane facing direction[15]. If the concentration of the immediate layer is lower than that of the external solutions, the ion-exchange layer which faces the concentrated solution will play the dominant role in determining the whole membrane potential, because the concentration ratio between the intermediate layer and the external concentrated solution is much higher than that between the intermediate phase and the external dilute solution.

According to evolving literature convention, a Bi-Polar membrane is in the (+) orientation when it's positively charged (anion-active) AEM layer is in contact with the more concentrated solution. Generally, the values of the concentration polarization E_c, consisting of two Donnan potentials on the two boundaries membrane-solution, are smaller with monopolar membranes and less positive with Bi-Polar membranes in the (+) orientation than the (-) orientation. In the (+) orientation, the overall charge and (and the E_c value) of a Bi-Polar membrane must be less positive than in the other because the

contact of the positively charged layer with the more concentrated solution leads to a screening of the positive charge by the electrolyte and vice versa.

2.6.2 Bi-Polar Membrane Water Splitting Discussion

It is well known that salts in solution can be converted unto their corresponding acids and bases by a process called electrodialytic water splitting across a Bi-Polar membrane. In the presence of a potential field, water at the interface will dissociate according to the following relation:

$$H_20 \leftrightarrow H^+ + OH^-$$

This water dissociation and its coupling with ion transport offer the possibility of using Bi-Polar membranes in a great variety of practical applications.

The process of electrodialytic water splitting consists of a Bi-Polar membrane arranged between two electrodes. If an electrical potential difference is established between the electrodes, charge species are removed from the interface between the two layers. When all the salt ions are removed from the solution between the two membranes, further transport of electrical charges can be accomplished only by the protons and hydroxide ions available from the ionization of water. Water so removed from the interface is replenished by water diffusing into the interface[16].

When no ions are available within this region, further transport of electric charge can be accomplished only by H^+ and OH^- ions, which are available even in completely desalinated water. At a theoretical potential of 0.828 V (see Section 2.6.2.1), the water in the AEM dissociates (splits) into equivalent amounts of H^+ and OH^- ions. These ions ideally migrate from the intermediate layer with the H^+ ions permeating through the CEM side and the OH^- ions permeating the AEM side. However, H^+ and OH^- ions are not very effectively retained by a Donnan potential and co-ion leakage of H^+ through the AEM as well as the OH^- leakage through the CEM can occur[7]. In addition, the H^+ leakage through the AEM will increase with the water content of the membrane.

In Bi-Polar membranes both the cation- and anion-exchange groups of the membrane polymer adjacent to the interphase layer can react with the water molecules. It is thought, however, that the water splitting reaction takes place primarily at the anionic surface[17]. One theoretical analysis suggests that water splitting in anion exchange membranes containing quaternary ammonium groups is due to the presence of tertiary alkyl amino groups in the surface regions that cannot bond with the water molecules. By contrast water splitting is not manifested by cation exchange membranes with sulphonic groups if the system is sufficiently clean[18]. Although the theoretical potential to achieve water dissociation is 0.828 V, the charged species within the intermediate layer are removed at a lesser potential and research is ongoing to determine if some H^+ and OH^- ion generation may occur at a lesser potential caused by direct membrane interactions.

2.6.2.1 Bi-Polar Membrane Water Splitting EMF Calculation

The conventional method for generating H^+ and OH^- ions from water utilizes electrolysis. Electrolysis also generates O_2 and H_2 gas, and the over voltage for this generation consumes about half of the electrical energy of the process. An alternative to this uses special ion-exchange membranes developed specifically for splitting water directly into $H^+ + OH^-$ ions without generating gases. Membrane water splitting technology is a general purpose unit for converting water-soluble salts to their corresponding acids and bases. The process uses Bi-Polar membranes in conjunction with conventional AEM/CEM under the presence of a direct current driving force for ion separation and rearrangement.

The water splitting process is electrodialytic in nature because the process merely involves changing the concentration of ions that are already present in solution. The theoretical energy for concentrating H^+ and OH^- ions from their concentration in the interface of the Bi-Polar membrane to the acid and base concentrations at the outer surfaces of the membrane can be calculated readily. The free energy change in going from the interior of the membrane to the outside is given by:

$$\Delta G = -nFE^{\circ} = -RT \ln ([(a^{i}_{H+} a^{i}_{OH-})/(ao_{H+} a^{o}_{OH-})]$$

Where a's are the activities of the H^+ and OH^- ions, superscripts i and o refer to the interface and outer surfaces of the membranes respectively. For generating one normal ideal product solution it reduces to (since n = 1) to:

$$\Delta G = -nFE^{\circ} = -RT \ln (a^{i}_{H+} a^{i}_{OH-}) \qquad \text{or} \qquad E^{\circ} = -RT/nF \ln K_w$$

and K_w is the ion-product or dissociation constant of water.

To overcome this potential, a potential $E = E_{cell} = -E^{\circ}$ must be applied across the membrane. Using the data on free energy for dissociation of water one can calculate the theoretical potential for generating acid and base for an ideal, i.e., perfectively permselective, Bi-Polar membrane as 0.828 V at 25C and 0.874 V at 70°C[19]. The actual potential drop across a Bi-Polar membrane is quite close to this being in the range of 0.9 – 1.1 V[3].

Using standard reduction potentials, E_{cell} and K_w can be calculated for $H_20 \leftrightarrow H^+ + OH^-$.

At the electrode surfaces the following half-cell reactions occur:

Anode (positive/right electrode): $2H^+ (aq) + e^- \rightarrow H_2(g)$ $\quad E^{\circ} = 0.000$ V

Cathode (negative/left electrode): $2H_20 (l) + 2e^- \rightarrow H_2(g) + 2OH\text{-} (aq)$ $\quad E^{\circ} = -0.828$ V

From which the standard EMF for this reaction can be calculated as:

$$E_{cell} = E^{o}_{Cathode} - E^{o}_{Anode} = -0.828 - 0 = -0.828 \text{ V}$$

and the ion-product or K_w calculated below from E_{cell} to be equal to 0.986×10^{-14} from

$$K_w = \exp (nFE_{cell}/RT) = [(1*96{,}500 \text{ C mol}^{-1} * -0.828) / (8.314 \text{ J K}^{-1} \text{ mol}^{-1} * 298\text{K})]$$

2.7 Electrodialysis

ED is the most common electro-membrane process used for desalination and concentrating of aqueous solutions. ED depends on the following general principles:

1) Most dissolved in seawater salts are ionic, being positively (cationic) or negatively (anionic) charged (See Table 2.2),
2) These ions are attracted to electrodes with an opposite charge,
3) Seawater is nominally 86% NaCl with Na and Cl nearly 100% ion free,
4) When NaCl is dissolved in water, it dissociates into hydrated Na^+ and Cl^- ions.

ED uses an electrical potential to move salts selectively through permselective membranes, leaving behind fresh product water.

ED is different from other desalination membrane processes in that it is electrically driven rather than pressure driven. Thus, in ED, only ions and associated

Table 2.2 Typical Seawater Composition

Major constituents in surface seawater*

Seawater TDS = 35,000 mg/l (ppm)
Typical Open Ocean pH = 8.2

		Atomic	Hydration	Ion	%	Concentration					
	Cation	Weight	Number	Charge	Ion Free	g/kg	mg/kg (ppm)	mol/g	mmol/kg (ppm)	meq/kg (ppm)	$CaCO_3$ meq
Sodium	Na+	22.9898	2	1	98- 99	10.781	10,781	0.4689	468.947	468.947	23447.35
Potassium	K+	39.0983	0.6	1	98-99	0.399	399	0.0102	10.205	10.205	510.25
Magnesium	Mg++	24.305	5.1	2	87-90	1.284	1,284	0.0528	52.829	105.657	5282.86
Calcium	Ca++	40.08	4.3	2	89-91	0.4119	412	0.0103	10.277	20.554	1027.69
Strontium	Sr++	87.62	3.7	2		0.00794	8	0.0001	0.091	0.181	9.06
Boron	B+++	10.81		3		0.0045	5	0.0004	0.416	1.249	62.44
	Anion										
Chloride	Cl-	35.453	0.9	-1	100	19.353	19,353	0.5459	545.878	545.878	27293.88
Sulfate	SO4--	96.0676		-2	39-54	2.712	2,712	0.0282	28.230	56.460	2823.01
Bicarbonate	HCO3-	64.0118		-1	69-80	0.126	126	0.0020	1.968	1.968	98.42
Bromine	Br-	79.904	0.9	-1		0.0673	67	0.0008	0.842	0.842	42.11
Fluorine	F-	18.9984	1.8	-1		0.0013	1	0.0001	0.068	0.068	3.42

*** An Introduction to the Chemistry of the Sea by M. E. Q. Pilson**

Total salt weight (gms)/Kg seawater =	35.15
% Monovalent Content =	86%
% Divalent Content =	13%

General Notes/Definitions

1. A one molar solution is prepared by adding one mole of solute to one liter of solution
2. Based on Boric Acid $[B(OH)_3]$ concentration of 0.0257 g/kg at 35 per mil salinity which does not ion pair
3. 1 ppm or 1 mg/kg is the lower limit of the major constitiuents which are mostly conservative
4. meq = milli equivelents = mol/g normalized by ion charge
5. 1 Liter = 1000 grams so meg/kg is also meg/Liter, similarly mmol/kg is also mmol/Liter
6. $CaCO_3$ meg is defined in terms of Alkalinity by mult meg/kg by 50 (the equivelent weight of $CaCO_3$)
7. What is the molarity of sodium chloride in seawater? Remember 1000g = 1 liter and a 1 molar solution is prepared by adding 1 mole of solute to 1 liter of solution
   10.781+19.353 = 30.134 gms of NaCl in seawater (86% of total salt). Mol wt of NaCl is 22.9898+35.453 = 58.4428 g/mol. Therefore, 30.134/58.4428 = .52 molar
8. What is the molarity of the water in seawater? Remember 1000g = 1 liter and a 1 molar solution is prepared by adding 1 mole of solute to 1 liter of solution
   1000 - 35.15 = 964.85 gms of H_2O in seawater. Mol wt of H2O is 1+1+15.99 =18.01528 g/mol. Therefore, 964.85/18.015= 53.56 molar or about 100:1 vs the NaCl

water is transferred. Cations, under the influence of the negative electrode move through the CEM but are stopped at the AEM interface. Similarly, anions under the influence of the positive electrode move through the AEM but are stopped at the CEM interface. In a typical ED configuration, AEM and CEM's are alternately arranged with a spacer sheet between to form a "cell". The basic ED unit consists of several hundred cell pairs bound together with electrodes on the outside and is referred to as a membrane stack. Pathways in ED units are separated by a cation/anion membrane stacks and direct current provides the motive force for ion migration from the low concentration side to the higher concentration side. By this arrangement, concentrated and diluted solutions are created in

the spaces between the alternating membrane pairs. Figure 2.4 presents a typical ED unit layout.

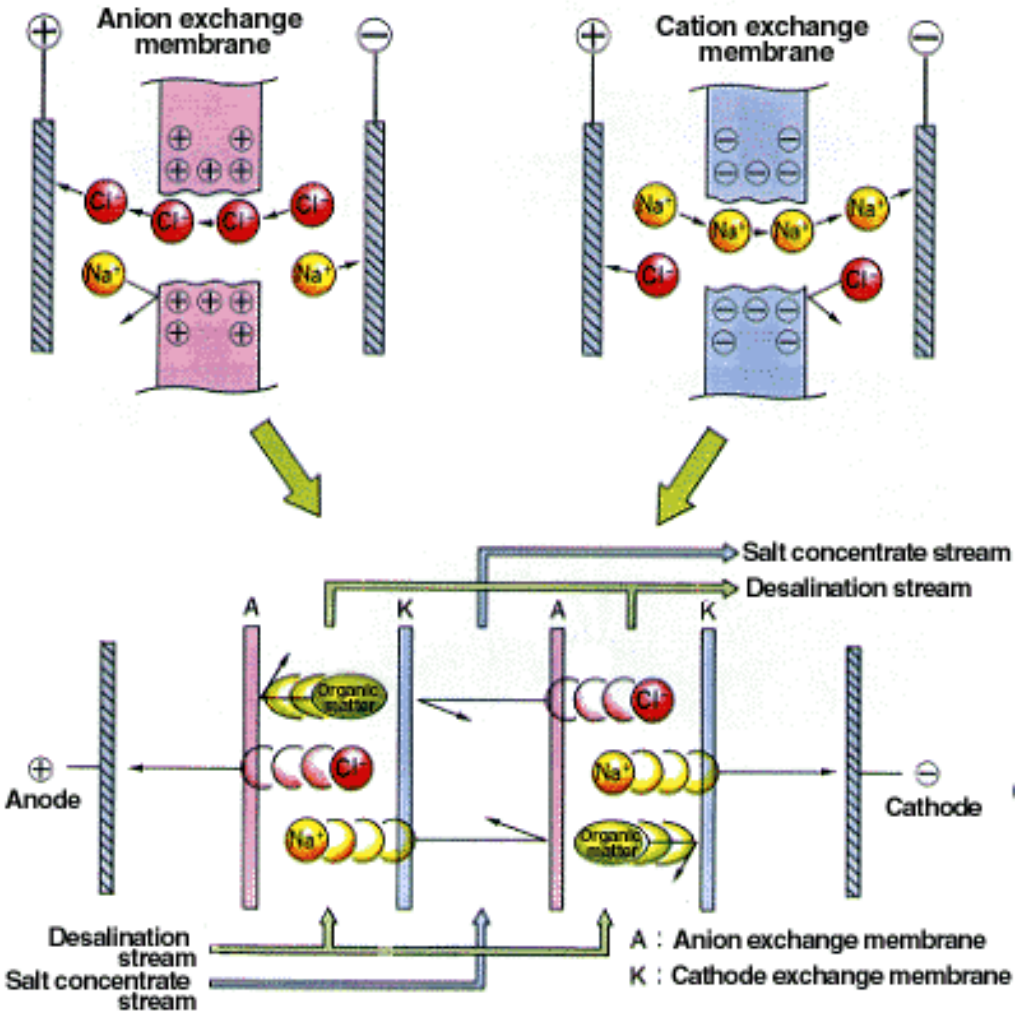

Figure 2.4 Typical Electrodialysis Unit Layout

2.8 Concentration Polarization Effects in Diffusive Membrane Systems

In pressure driven processes such as Reverse Osmosis (RO), Microfiltration (MF) and Ultrafiltration (UF), solutes are retained to some extent by the membrane. In this way the solute concentration profile has been established by the convective flow towards

the membrane and the diffusive back transport of the solute towards the bulk. In ED units, adjacent fluid pathways are separated by a cation/anion membrane stack where applied direct current provides the motive force for ion migration. In these cases, concentration polarization and boundary layer effects can be significant.

In ED application, the solution compartments and membranes, being in series, must carry the same electrical current. In the solution compartments, both the cations and anions carry the current. In the membranes, however, only one type of ion (cation or anion) can do this. Therefore, the ions in the membranes must travel at twice the speed that they move in the bulk solution compartments. This causes the concentration of the ions to be depleted on the entrance side of the membrane in comparison with the concentration in the bulk solution. This concentration polarization requires a higher current to transport the ions. If the current is increased to the critical point i_{lim} – at which the membrane surface on the entrance side is totally depleted of ions (cations or anions) – two results follow:

1) An increase in the resistance considerably boosts energy consumption,
2) H^+ and OH^- ions are transported across the membranes, and water is dissociated.

The transport of H^+ and OH^- ions result in locally high and low pH levels at the membrane surfaces[20]. The locally high pH on the brine side can cause salts with limited solubility such as $CaSO_4$ and $CaCO_3$ to precipitate[19]. The limiting current, the current at the critical point, $i_{lim,}$ is directly related to: (1) the concentration of the ions in the bulk

solution (the limiting current is smaller for a lower total-dissolved-solids solution), and (2) the thickness of the boundary layer.

However, in purely diffusive driven systems such as concentration cells, preferential ion transport occurs through the membrane according to the internally generated driving force with the concentration of solute at the membrane surface dependant upon the flux through the membrane, membrane retention, the diffusion coefficient of the solute D, and the thickness of the concentration boundary layer d, *i.e.*, the region near the membrane in which the concentration of solute varies. Because of current densities generally below i_{lim}, low transport rates, and low solute mass transfer rates, it is frequently assumed that the resistance to ion transport in concentration cell systems is determined primarily by the membrane phase with boundary layer resistances neglected[5].

2.9 Osmosis

Osmosis is the phenomenon of water, solvent, flow through a semi-permeable membrane that blocks the transport of salts (solute). With membranes which are nonionic or completely impermeable for the solute, the solvent flux is from dilute to the concentrated solution and is proportional to the osmotic pressure difference between the two solutions. This pressure difference occurs whenever a membrane separates a solvent from a solution and is given almost entirely by the total concentrations of the dissolved species (ions or molecules) and depends very little on the individual species.

2.9.1 Anomalous Osmosis Basics[21]

Solvent diffusion, osmosis, across an ion-exchange membrane is, as a rule, anomalous, i.e., not proportional to the osmotic pressure between the solutions. The pore liquid in the membrane carries a net electric charge and, hence, is affected by the both the pressure gradient and the electric potential gradient which arises from ionic diffusion.

The effect of the pressure gradient alone always results in Positive Osmosis. The swelling pressure, i.e., the pressure difference between the ion-exchange membrane and the equal hydrostatic pressure, is higher on the side of the dilute solution (higher free energy) and drives the solvent toward the concentrated solution side.

The effect of the pressure may be enhanced, partly balanced, or even out weighed by the electric field. Strong diffusion potentials arise when the mobility of the counter ion and co-ion differ greatly. If the counter ions are faster, the resulting electric field – in addition to enforcing equivalence of the ionic fluxes – drives the electrically charged pore liquid as a whole toward the concentrated solution. The effect of the electric field thus adds to that of pressure and produces Anomalous Positive Osmosis. However, if the co-ion is faster, the electric field has opposite sign and drives the pore liquid toward the dilute solution. The electric field may be stronger than the pressure. In this case there is Anomalous Negative Osmosis. Here, solvent diffusion provides the energy required for transferring the electrolyte against its chemical potential gradient. The described anomalous phenomena only apply to the solvent.

The transport of solvent (water) through the membrane is a critical factor determining the performance of fuel cells, and the water balance between anolyte and catholyte is important in many applications of electrolysis, determining for example the maximum concentration of product which can be achieved. Besides the pressure and chemical gradients discussed, water passes through the membrane with the ions within their hydration shells, i.e., electro-osmosis.

Chapter 3

Initial Phase I Investigation and Discussion

3.1 Technical Background and Discussion

A primary driving force behind the industrial development of membranes has been desalination for municipal drinking water supplies where ED and RO have been used for water desalting. More frequently, desalination plants are being co-located near power generation stations such that power plant discharge cooling water of elevated temperature and thus increased ion-mobility becomes the desalination plant source water. High TDS RO waste stream concentrate is then available for additional processing to allow economic recovery and reuse of the energy in the waste stream. Sources of dilute brine include brackish river/estuarine water or treated municipal water (also typically co-located). In order to capture the energy of this potentially significant energy source, a suitable energy extraction device must first be developed.

3.1.1 General Ion-Exchange Electro-Membrane Theory Discussion

The heart of any electro-membrane process is the ion-exchange membrane. It usually consists of a polymer film with ionic groups attached to the polymer backbone. As mentioned in Chapter 2, if these "fixed charges" contain a negatively (anionic) charged group fixed to the polymeric chain they are called a CEM because they are

capable of exchanging positively charged cations. When the fixed charged group is positive (cationic), the membrane is called an AEM because it is capable of exchanging negatively charged anions. In the case of cationic fixed charges, the freely moveable counter-ions are anions. The membrane, therefore, exhibits ion-exchange properties for counter-ions, which can permeate the membrane easily and excludes co-ions (of the same charge as the fixed charges) from the passage. The "permselectivity" between counter- and co-ions can reach values up to 99%. The permselectivity decreases with increasing ion concentration of the outside solution and decreasing capacity and degree of cross linking of the ion-exchange membrane. All electro-membrane processes make use of the above permselectivity of ion-exchange membranes[3].

An electric field in an electrolyte solution produces transference of ions whose transport across an ion-exchange electro-membrane. In a solution of uniform composition under the assumption of electro-neutrality, the transference of an arbitrary ionic species in the direction of the current is proportional to the gradient of the electric potential, the concentration difference, and the electrochemical valence of the ionic species. It is irrelevant whether the field is generated by an external source (as in ED) or generated internally via concentration gradient driven diffusion, since the individual ion has no means of knowing the origin of the electric field[6].

Electric current in an ion-exchanger transfers predominantly via counter-ions by diffusion. The co-ion has relatively little effect on the kinetics and the rate of ion exchange. The Nernst equation holds reasonably well within the concentration range of

about 10^{-4} to 10^{-1} N for estimations of OCV. Deviations at higher solution concentrations are caused by co-ion transference, and at lower concentrations by H^+ (protons) or OH^- (hydroxyl) ions (stemming from dissociation of H_20) that compete with the electrolyte counter ion (*i.e.,* the increasing concentration of the co-ion in the ion exchanger causes a decrease in the transport number of the counter-ion). As discussed in Section 2.5.1, the limiting OCV value of the membrane potential (at room temperature) is 0.059 V per power of 10 activity ratios using a single ideal monopolar membrane, a 1,1 valence electrolyte, and reversible electrodes[4]. This cell membrane potential may be higher if the co-ion is more mobile than the counter-ion and if there is little Donnan exclusion of the co-ion[6].

3.1.2 Relevant Related Work

Although numerous authors have written on the subject of non-replenishing concentration cells, Ohya's[22] test configuration using a single pair of anion/cation monopolar semi-permeable membranes separated by a center region is particularly relevant. Ohya reported maximum cell OCV values of nominally 0.100V after several hours before dropping off. Ohya theorized that the reason for this OCV build up and drop off might be that as time passed, the center compartment concentration increased with a corresponding decrease in electrical resistance, resulting in an increase in the observed OCV. However, as the center compartment's concentration continued to increase, the relative concentration between the center and either side decreased with a corresponding decrease in the cell's potential. This should not be the case in a

replenishing Bi-Polar membrane concentration cell design and to the author's knowledge there is no comparable research or technology currently operating on this unique concept.

3.1.3 Bi-Polar Membrane Discussion

An extensive literature and membrane evaluation review revealed the presence of Bi-Polar membranes. A Bi-Polar membrane consists of a monopolar CEM and monopolar AEM joined together with an intermediate transitional phase layer in between. Although made up of well-defined components, once combined the Bi-Polar membrane acquires unique capabilities and additional uses. These include: 1) an apparent variation in membrane potential depending upon which side is in contact with the more concentrated solution, which is not the case in monopolar ion-exchange membranes[14]; 2) its use in converting water-soluble salts to their corresponding acids and bases via the process of water dissociation (or splitting). Where H^+ and OH^- ions, removed from the transitional phase layer, are replenished by water transported into the membrane[2].

These additional and unique benefits coupled with Ohya's findings led me to Bi-Polar membrane concentration cell testing rather than continuing with the typical ED based anion/cation monopolar membrane stack arrangements. As is the case with standard AEM/CEMs, when an electrical field is established across a Bi-Polar membrane the transfer of electrical charge will be carried preferentially by the ions present. However, under the effect of an electric field, charged species are also removed from the transitional phase layer between the two ion-exchange layers.

When no ions are available within this region, further transport of electric charge can be accomplished only by H^+ and OH^- ions, which are available even in completely desalinated water. At a theoretical potential of 0.828 V, the water in the transitional phase layer dissociates (splits) into equivalent amounts of H^+ and OH^- ions. These ions ideally migrate from the intermediate layer with the H^+ ions permeating through the CEM side and the OH^- ions permeating the AEM side. However, H^+ and OH^- ions are not very effectively retained by a Donnan potential and co-ion leakage of H^+ through the AEM as well as the OH^- leakage through the CEM can occur[7].

3.2 Test Results and Recommendations

An initial baseline, bench top, proof-of-concept laboratory test apparatus was constructed, see Figure 3.1. It consisted of a single concentration cell of cubic design, a peristaltic pump, and a computer running a data acquisition program. The test cell consisted of two symmetrical sections (a concentrated solution side and a dilute solution side) separated by a single Bi-Polar membrane. Each section consisted of an end plate, electrode, and test chamber. The concentrated ionic solution side consisted of an entrained saturated slurry reservoir. 1:10 ionic test solutions were made from dilutions of the saturated concentrate. The dilute solution was pumped through the dilute cell side and collected in a 1,000 ml beaker. Measurements of the dilute input/output ionic test solution salinity revealed higher levels of Cl^- in the output solution corresponding to possible CEM co-ion migration (lower anion permselectivity). Low cation AEM

permselectivity may also be present but measurements were not made for specific cations, nor were they made for solution pH, or the presence of multi-valence ions.

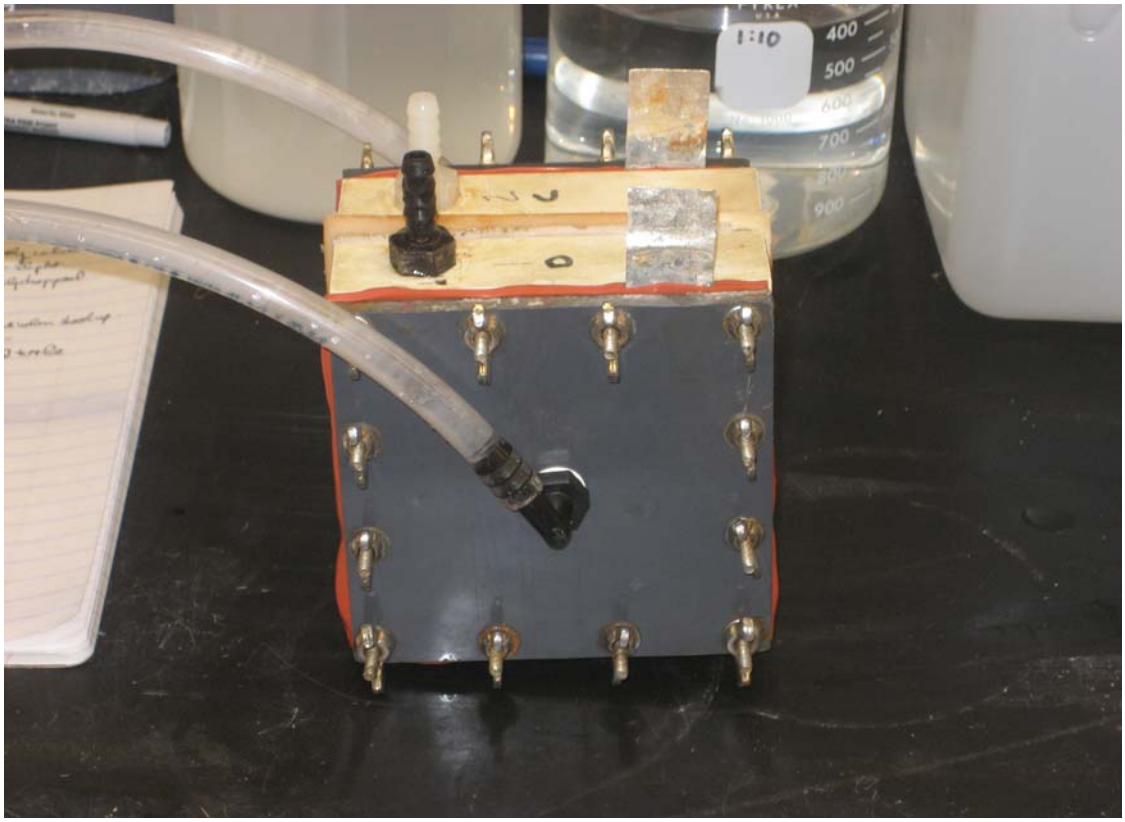

Figure 3.1 Standard Bi-Polar Membrane Concentration Test Cell

OCV and various loaded voltage measurements were made with a computer running a data acquisition program. Figure 3.2 below shows a result from one of the test configurations using a Bi-Polar membrane in the (+) orientation. Note the battery like performance including a possible Coup de Fouet effect occurring just after initial discharge. As can be seen in Figure 3.2, the OCV value measured was several times that predicted by the Nernst equation and more than twice that reported by Ohya, although measurements made under electrical loading were significantly lower in value.

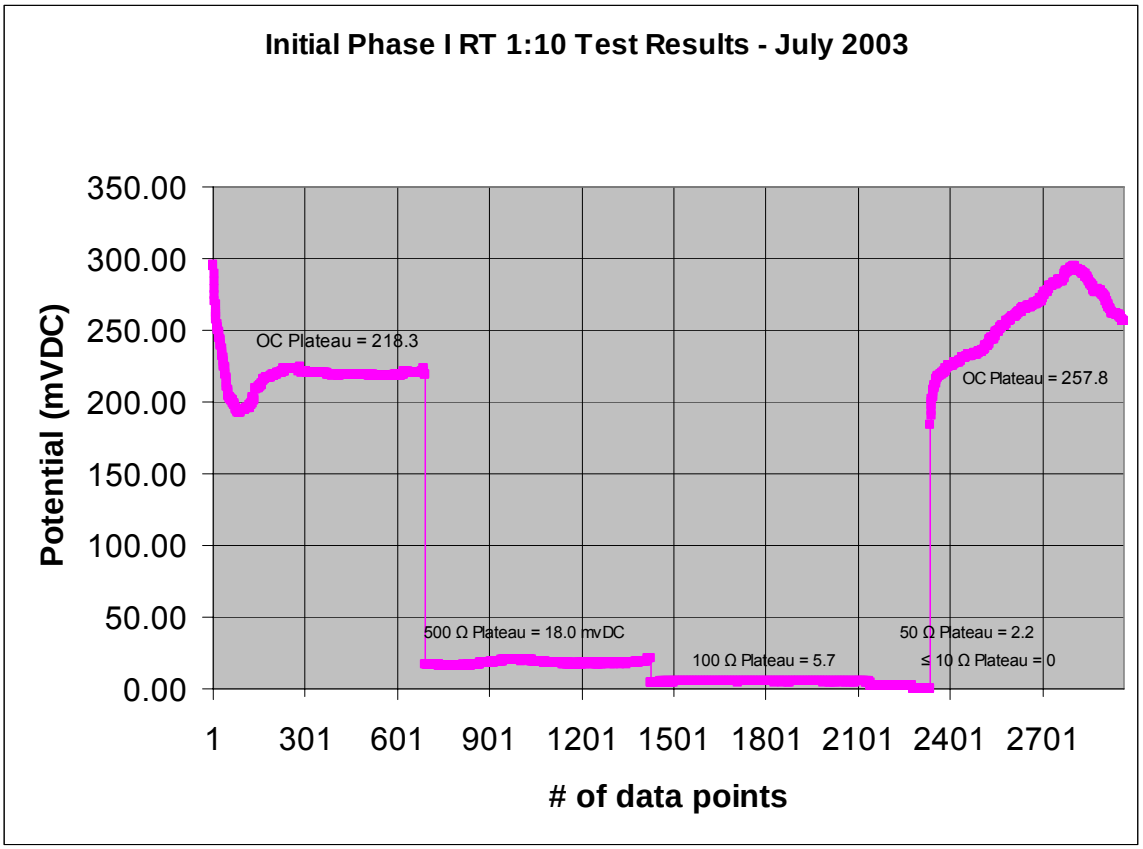

Figure 3.2 Bi-Polar Membrane Concentration Cell Proof-of-Concept Test Results

Although small in value, the measured cell membrane potentials were in the realm suitable for low power energy harvesting or MEMS applications. Based on these favorable results, a more thorough testing program using a consistent test configuration subject to changing membrane/electrode parameters and ionic/environmental effects was devised and implemented. Additional research was conducted in order to investigate and evaluate the membrane potential generation in a Bi-Polar electro-membrane based seawater concentration cell and its suitability as a low power energy source for energy harvesting/MEMS devices. Included in this test effort was electrochemical testing and modeling required to determine an equivalent cell circuit design impedance for maximum power delivery, via impedance matching, to a coupled electrical device. This phase II

detailed test discussion is presented in Chapter 4. Phase II testing methodology, results and analysis are presented in Chapter 5, followed by a contribution and future research recommendations summary in Chapter 6.

Chapter 4

Detailed Phase II Test Discussion

4.1 Overview and Purpose

As discussed in Chapter 3, a phase I proof-of-concept Bi-Polar membrane based concentration cell was built and tested with the measured OCV values several times the value predicted by the Nernst equation and more than twice that reported by Ohya, although measurements made under electrical loading were significantly lower in value. The initial proof-of-concept test apparatus was a single cubic shaped cell, but other geometries are possible depending upon the end use. Further, although a single cell was initially tested, it is envisioned that in actual use a plurality of cells will be aligned in series/parallel configurations to generate the desired output power. In addition, a variety of differing cell designs may also be included within the array structure, such as an annular design suitable for inclusion into a high flow rate power plant or desalination plant application, designs including ion exchange resins or conductivity enhancing materials, and designs combined with monopolar membranes.

The broad use of options permits a wide variety of applications for the instant power generating system, with controls being devised by the types and numbers of cells

in the generating array. This dissertation provides documentation detailing the testing results along with analysis and recommendations, serving as a baseline for full-scale testing during later phases of this technology development.

4.2 Research Objectives

The over arching research goal is to provide a contribution to the body of knowledge as well as to suggest one solution to the engineering problem of how to extract useful energy from available dilute and concentrated saline solutions. This exploratory research effort consisted of several major areas:

1) Determination of membrane/electrode processes and kinetics,
2) Equivalent circuit component modeling,
3) System wide cell performance testing,
4) Determination of cell parameter inter-relationships,
5) Examine the feasibility of this Dialytic based membrane concentration cell as a low power energy source for energy harvesting/MEMS devices.

4.3 Testing Summary

This Phase II testing effort consisted of an extended testing/monitoring program designed to determine OCV and loaded voltage and current output vice parameters such as: external electrical loading; temperature; pH, solution concentration, membrane selection and orientation, and electrode surface area. To minimize membrane and

electrode fouling effects, synthetic seawater solutions were used and the results compared. Close inspection of the test set up, membrane, and electrodes were conducted during the testing period including the use of a Scanning Electron Microscope (SEM) to ascertain membrane and electrode state of health. Detailed ion-transfer across the Bi-Polar membrane was analyzed by frequent Cl^- ion titration of solution samples removed from each side of the test cell at various times during the test runs.

Electrochemical methods such as Cyclic Voltammetry (CV) and Electrochemical Impedance Spectroscopy (EIS) along with equivalent circuit modeling were used to establish electrode processes and kinetics corresponding to changes in operating parameters. Statistical Design of Experiment (DoE) methods were used to investigate various parameter interactions. Cell performance testing consisted of the standard baseline proof-of-concept cell design operated over various test factor variable configurations. MEMS based application considerations were then considered in the latter part of the Phase II effort.

Chapter 5

Detailed Phase II Test Results and Analysis

5.1 Specific Test Methodology and Details

To examine performance, the Phase I **s**tandard Bi-Polar membrane concentration test cell was run for various periods of time and loading conditions and the results compared. The standard atmospheric pressure testing effort consisted of a monitoring program designed to determine OCV and loaded cell membrane potential voltage and current vice the following input parameters:

1) Synthetic seawater solution temperature (5 to 40 °C, nominally),
2) Synthetic seawater solution concentration differences (e.g., 1:10, 1:100),
3) Bi-Polar membrane end use differences (e.g., industrial electrochemical plating vs. water purification ED),
4) Solution pumping speed (Fisher Scientific low flow peristaltic pump 13-876-1),
5) Bi-Polar membrane orientation,
6) Silver (Ag) wire mesh electrode surface area.

Room temperature CV and EIS measurements were conducted over a frequency range of 10 MHz to 1 mHz using a Solartron SI 1260/1287 Frequency Response Analyzer and supporting test equipment to establish electrode, membrane, and full cell component characterization. This testing occurred at the University of South Florida's (USF) Corrosion Engineering Laboratory (Tampa, FL, ENL 111, Dr. Alberto Sagüés) and the University of Kentucky's Center of Applied Energy Research (Lexington. KY, Dr. Stephen Lipka). Figure 5.1 shows EIS testing at USF's Corrosion Engineering Laboratory.

Figure 5.1 EIS Testing at USF's Corrosion Engineering Laboratory

Full Cycle temperature and external electrical loading performance measurements were conducted using a using a hand held data logger (Vernier Software and Technology), computer, and supporting test equipment to establish cell membrane output

potential characterization. This testing occurred at the University of South Florida's (USF) College of Marine Science (CMS) (St. Petersburg, FL, KORC 2129, Dr. Luis García-Rubio). Figure 5.2 shows performance testing at the USF CMS.

Close inspection of the test set up, membrane, and electrodes were conducted during the testing period. SEM and X-Ray imaging techniques were used to ascertain membrane and electrode state of health. Bi-Polar membrane from several manufactures were obtained and used during the testing period for comparison. Specific membrane details came from the manufacturer and literature, as available, supplemented by testing.

Figure 5.2 Cell Performance Testing at USF's College of Marine Science

Because of the number of cell components and their coupled parametric interactions, it was desirable to characterize each individually and determine their respective interactions using Design of Experiment (DoE) and analysis techniques via Statistical Analysis System's (SAS) statistical analysis package. EIS impedance plots and cell Equivalent Circuit Modeling was analyzed using Solartron's ZView2 software package by Scribner Associates, Inc.

5.1.1 Synthetic Seawater Solution Discussion

Instant Ocean® Synthetic Sea Salt, made by Aquarium Systems, was used throughout this testing effort to provide a suitable medium for a seawater concentration cell with out the sometime deleterious effects of marine biofouling. Test solutions along with nominal Cl^- titration and pH measurement values were made as follows:

1) Concentrated Test Solution: 300 grams of Instant Ocean® added to enough Deionized (DI) water [Millipore Milli-Q 18.2 MW*cm] to make 1 liter of total solution. pH = 8.1 and Cl^- = 3.62M (N),
2) 1:10 Test Solution: 100 ml of concentrated test solution added to 900 ml of DI water. pH = 8.8 and Cl^- = 0.45M (N),
3) 1:100 Test Solution: 100 ml of 1:10 test solution added to 900 ml of DI water. pH = 9.0 and Cl^- = 0.05M (N).

Although a 1:10 concentration difference exists between 1 to 2 and 2 to 3, their Molarities differed by 8:1 and 9:1, respectively, which concurs, based on their respective activity coefficients and concentration values. Visual examination of the actual test solutions reveal a white, saturated Calcium Carbonate ($CaCO_3$) precipitate present in the concentrated test solution, however, the 1:10 and 1:100 solutions were clear.

5.2 Electrode Discussion

5.2.1 Electrode Details

In order to allow for the sole evaluation of the Bi-Polar membrane in the seawater concentration cell, the electrode material was carefully selected so as to only act as a charge collector. The chosen electrodes were made from standard silver (Ag) wire mesh with a solid Ag tab soldered for good electrical conduction and increased clip test lead attachment longevity. Initial surface treatment included a 20 minute dip in 3M HCL followed by a deionized water rinse. Electrode overall cross section is 3 inches by 3 inches with 2.75 inches by 2.75 inches in solution contact. Figure 5.3 presents a pair of used 80 Mesh electrodes.

Two sizes of mesh were used in the testing effort, one with 80 threads per inch and one with 40 threads per inch, in order to examine any electrode surface area depenendancy. Based on a cylindrical surface area estimation of each wire multiplied by

the number of wires, the 40 Mesh electrodes should have 11% more surface area than the 80 mesh electrode.

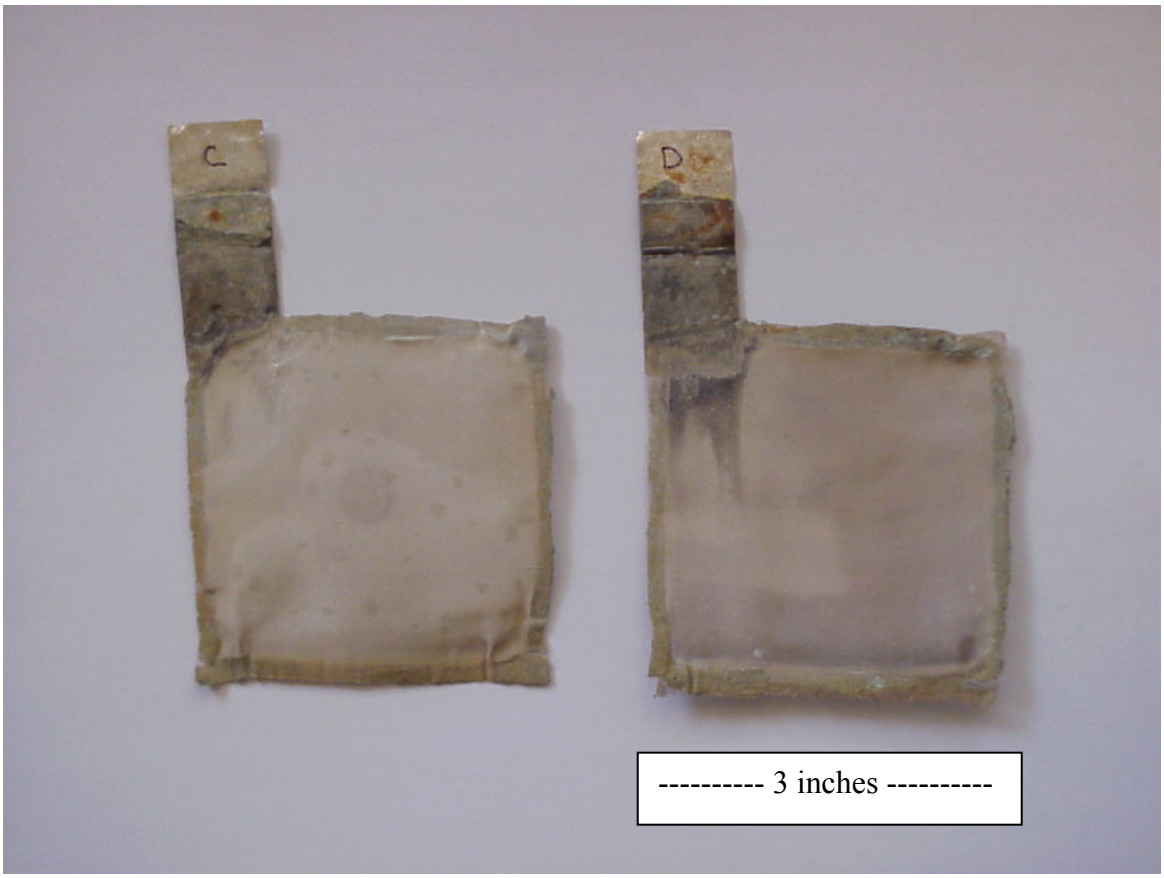

Figure 5.3 Used 3M HCL Dip 80 Ag Mesh Electrodes

5.2.2 Scanning Electron Microscopy and X-Ray Results

Figures 5.4 and 5.5 present SEM and X-Ray results, respectively, for a section of new 3M HCL dipped 80 Ag wire mesh. In the area X-Rayed, analysis revealed >96% of the total net counts in the X-Ray spectrum were Ag, as expected, with trace elements

present of C, Mg, Al, Cl and Si. These results were consistent with those found in a similarly sampled section of new 3M HCL 40 Ag wire mesh.

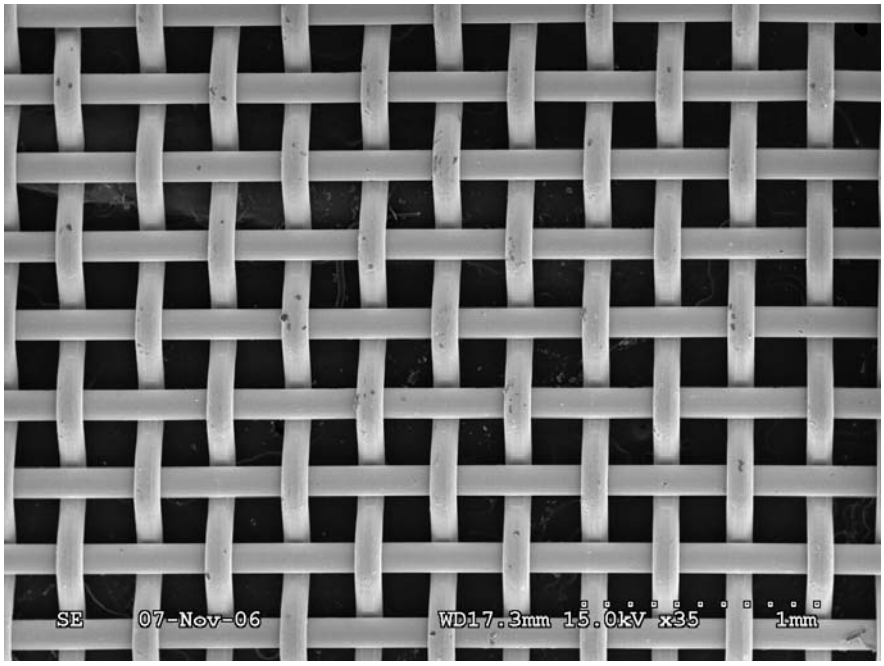

Figure 5.4 New 3M HCL Dip 80 Ag Mesh SEM

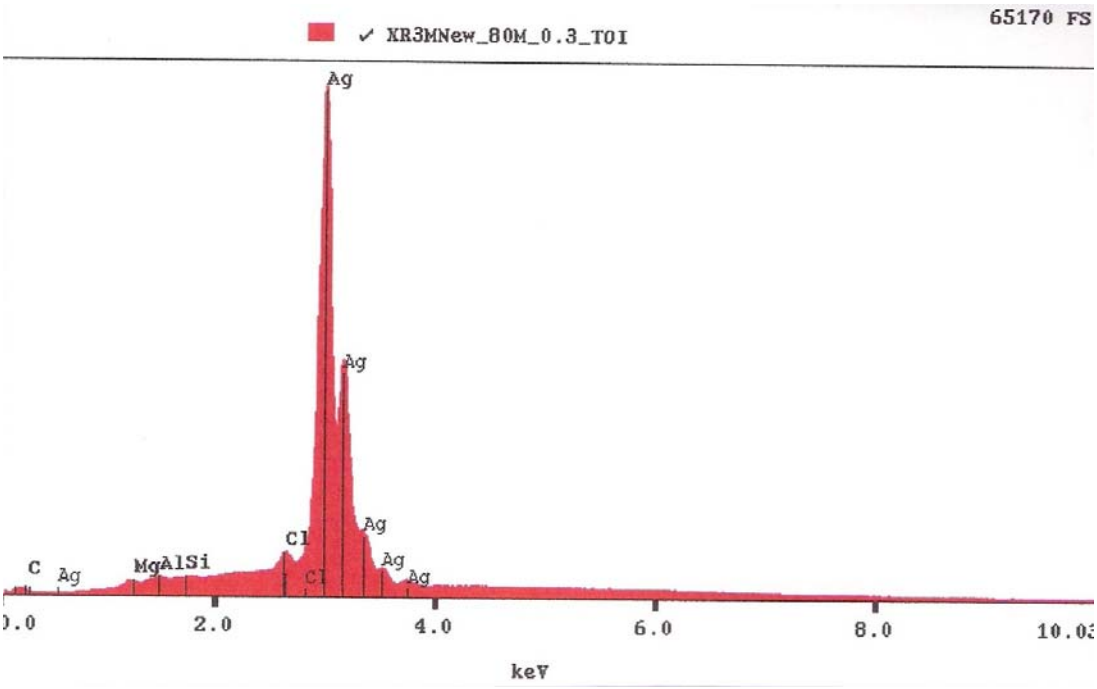

Figure 5.5 New 3M HCL Dip 80 Ag Mesh X-Ray

Figures 5.6 and 5.7 present SEM and X-Ray results, respectively, for a section of used 3M HCL dipped 80 Ag wire mesh electrode from the concentrated solution side near the cell top. In the area X-Rayed, analysis revealed >97% of the total net counts in the X-Ray spectrum were Ag as expected with trace elements of O, Mg, Na, and Cl present. These results were consistent with those found in a similarly sampled section of a used 3M HCL dipped 80 Ag electrode from the dilute solution cell side.

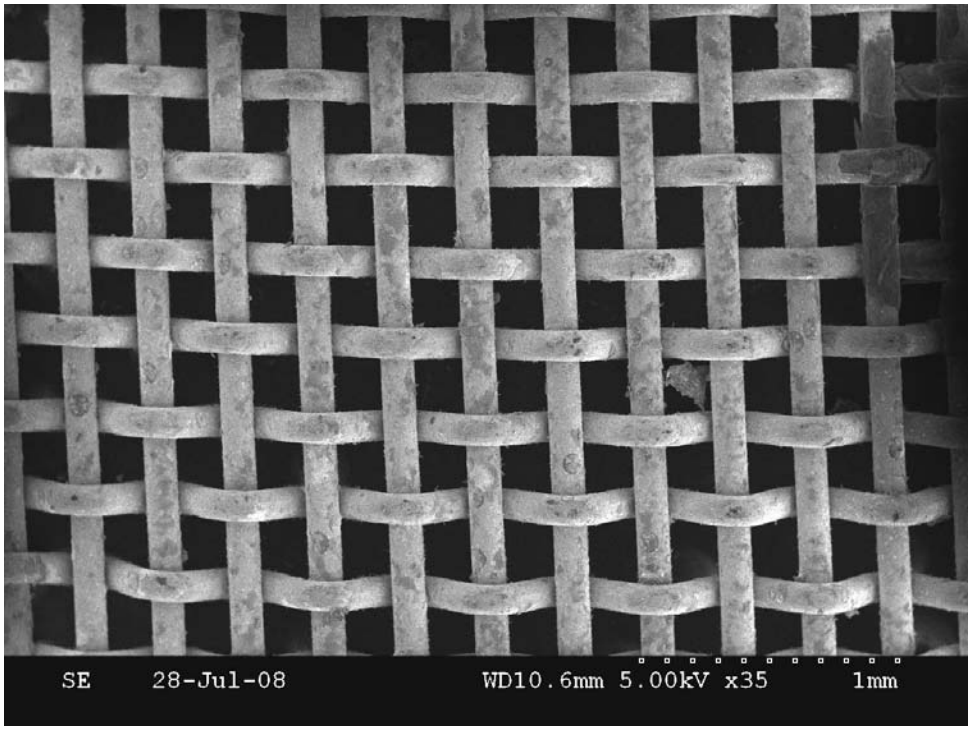

Figure 5.6 Used Electrode SEM Results from Concentrated Side Cell Top

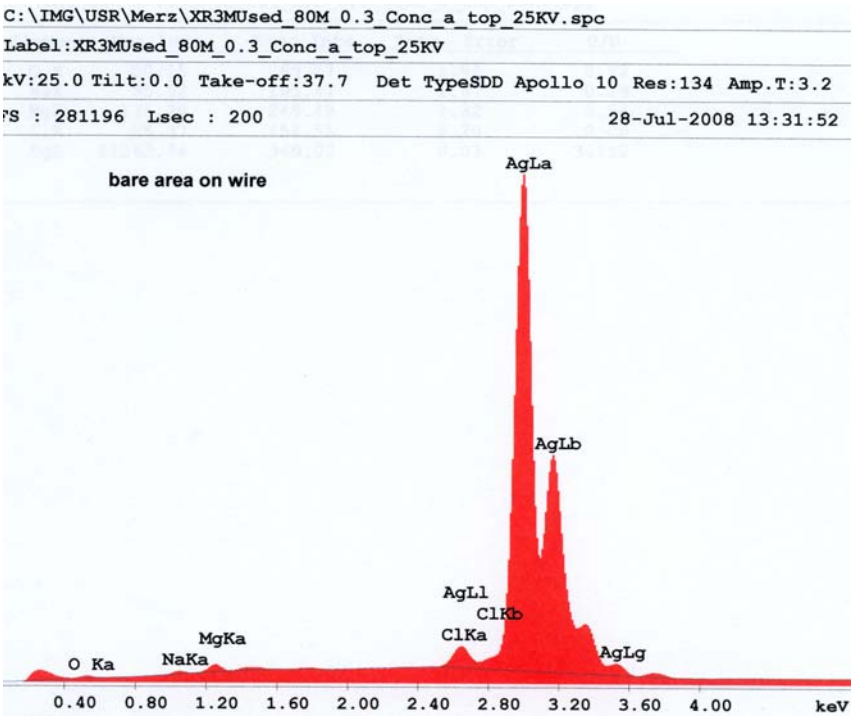

Figure 5.7 Used Electrode X-Ray Results from Concentrated Side Cell Top

Figures 5.8 and 5.9 present SEM and X-ray results, respectively, for a section of used 3M HCL dipped 80 Ag wire mesh electrode from the concentrated solution side near the cell bottom. Precipitated Ca crystals are clearly seen formed on portions of the imaged wire. This concurs with the previously noted observation of a white, saturated Calcium Carbonate ($CaCO_3$) precipitate in the 3.6M concentrated test solution.

In the shinny metal area X-rayed, analysis revealed >75% of the total net counts in the X-Ray spectrum were Ag with Ca (10%) and trace elements of O, Mg, Si, S, Na, Al, and Pb. X-Ray analysis on the precipitated coated wire reveal >83% of the net counts in the X-Ray spectrum, primarily Ca with trace elements of O, Sr, S, Cl, Mg, Ag, and Na.

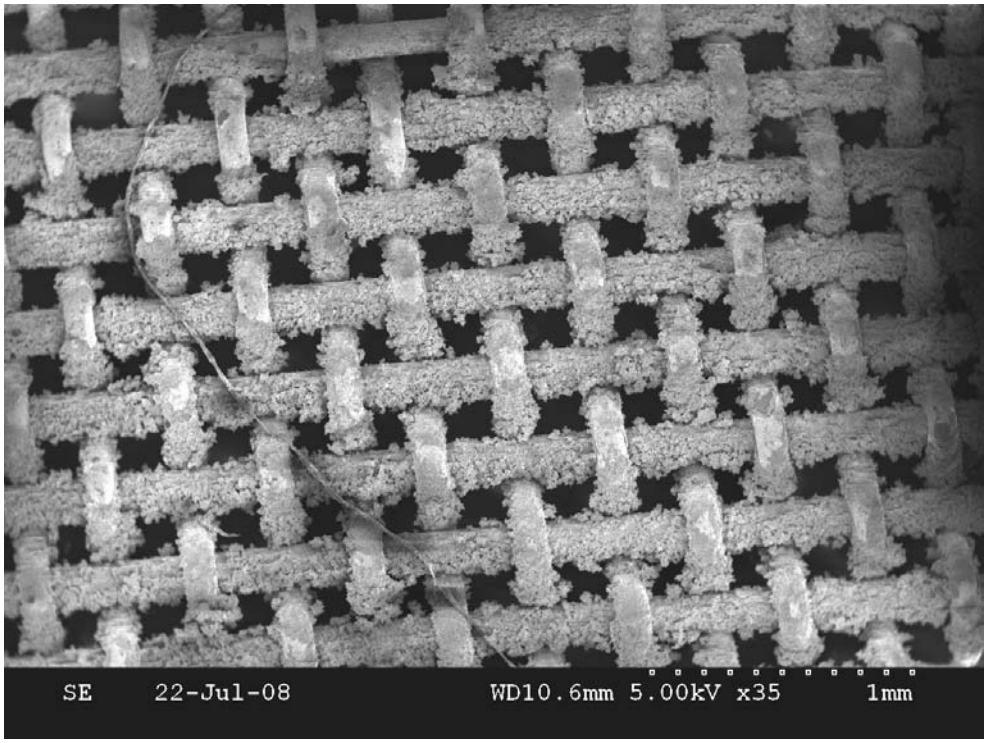

Figure 5.8 Used Electrode SEM Results from Concentrated Side Cell Bottom

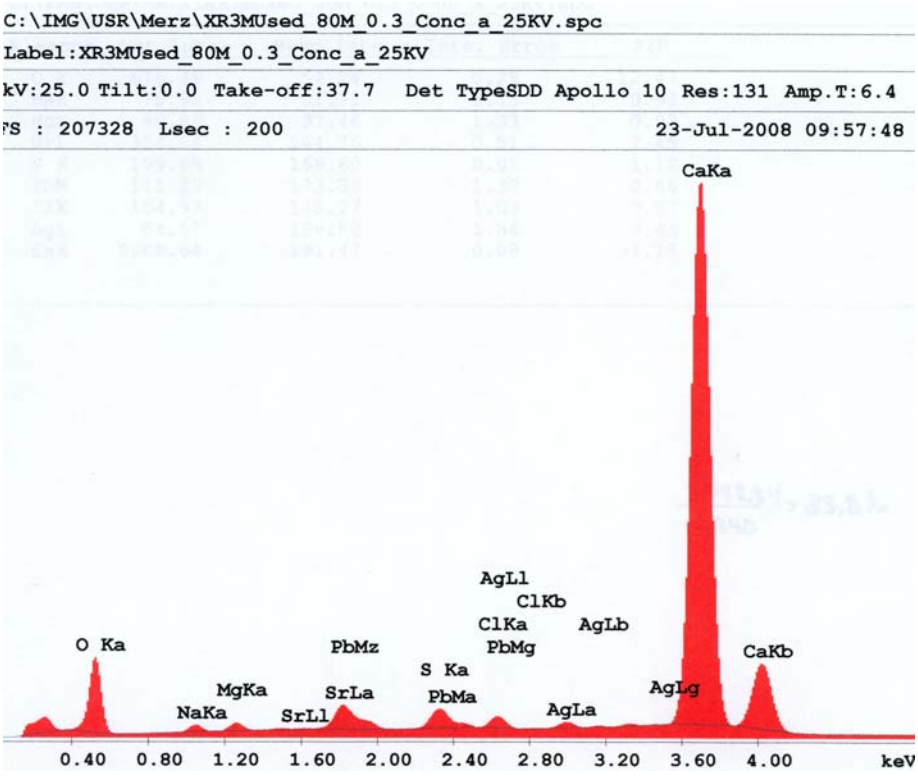

Figure 5.9 Used Electrode X-Ray Results from Concentrated Side Cell Bottom

Figures 5.10 and 5.11 present SEM and X-Ray results, respectively, for a section of used 3M HCL dipped 80 Ag wire mesh electrode from the dilute solution side near the cell bottom. In the bare wire area X-Rayed, analysis revealed >88% of the total net counts in the X-Ray spectrum were Ag with trace elements of Mg, O, Mg, Na, and Cl present. X-Ray analysis on the precipitate in the upper left corner revealed NaCl (>98%) with trace elements present of O, Mg and Ca.

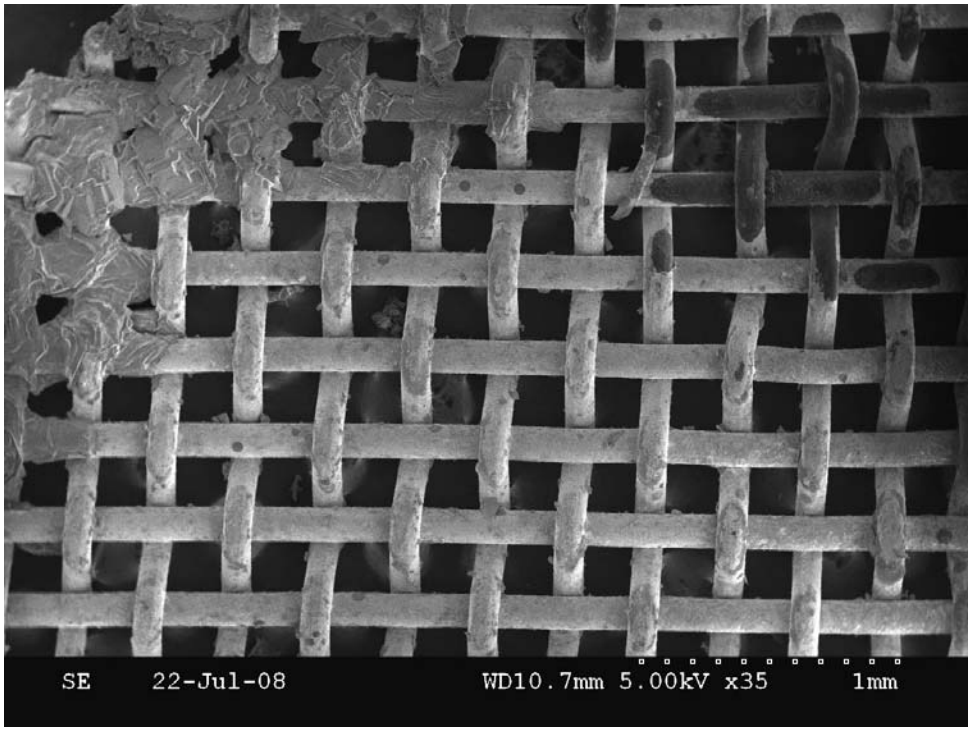

Figure 5.10 Used Electrode SEM Results from Dilute Side Cell Bottom

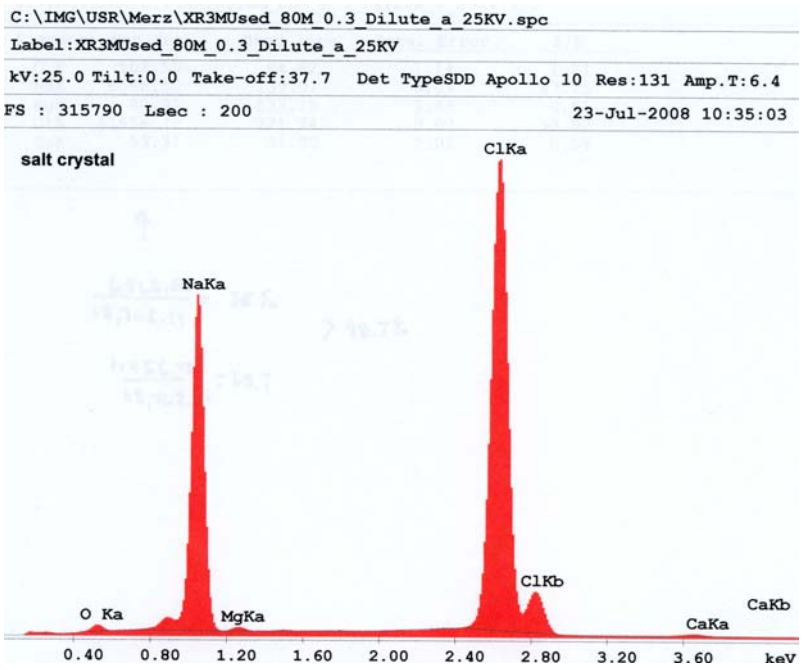

Figure 5.11 Used Electrode X-Ray Results from Dilute Side Cell Bottom

5.2.3 Cyclic Voltammetry Test Results

Many electrode reactions can proceed either as oxidation or as reduction, depending upon on the direction of the current flowing through the electrode/electrolyte interface, e.g., metal deposition/dissolution or Reduction/Oxidation (RedOx) reactions. Metal deposition/dissolution is a class of electrode reactions involving RedOx of a solid metal and its dissolved ion, e.g., where Ag ions can be cathodically reduced to Ag metal, or the Ag metal can be anodically oxidized to Ag ions. Compare with a RedOx reaction where both the oxidized and reduced species are in solution.

Voltammetry is an electrochemical measuring technique used for the determination of chemical reaction rates and their causes, kinetics, along with electrode

reaction mechanisms at the electrode surface. CV is a commonly used variation of the technique in which the direction of the working electrode potential is reversed at the end of the first scan all while the current flowing through the electrode is measured. CV has the advantage that the product of the electron transfer reaction that occurred in the forward scan can be probed again in the reverse scan.

The waveform used in this analysis is composed of two isosceles triangles and is presented in Figure 5.12 below[23]. Operation begins by first holding the initial potential where no electrolysis occurs and hence no faradaic current flows. As the voltage is scanned in the positive direction any reduced compound is oxidized at the electrode surface. At (+ve), the scan reduction is reversed and the material that was oxidized in the positive scan is then reduced. Once the voltage reaches (–ve) it is then retuned to the initial value. This operation is then repeated until repeatability is achieved.

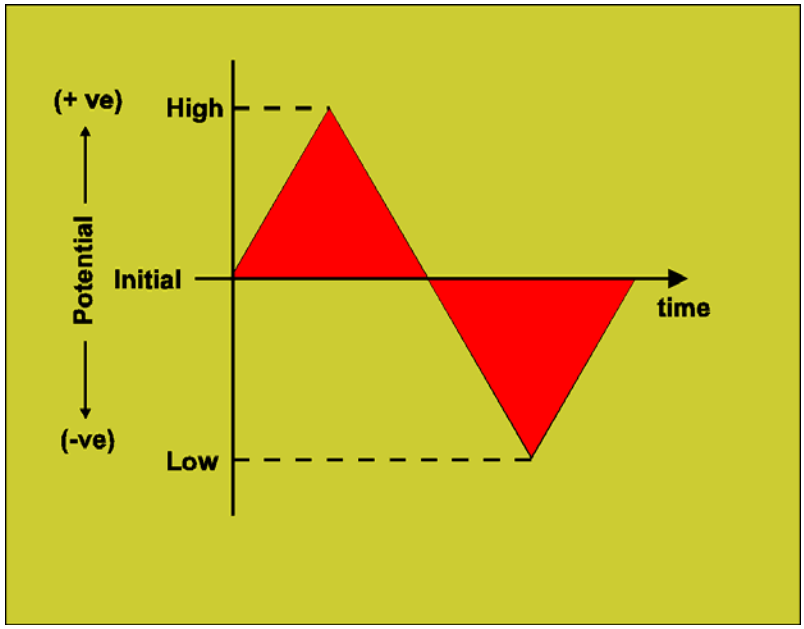

Figure 5.12 Waveform Used in CV Testing

CV testing was conducted on both new and used Ag 80 mesh electrode samples and a summary plot is presented in Figure 5.13. Examination of Figure 5.13 reveals that within the potential range typically encountered in an electrically loaded cell condition, the curve shape is flat with no transfer of charge occurring at the electrode. Supporting the original hypothesis that the electrodes would not be a contributor to the overall cell potential at the working voltages encountered.

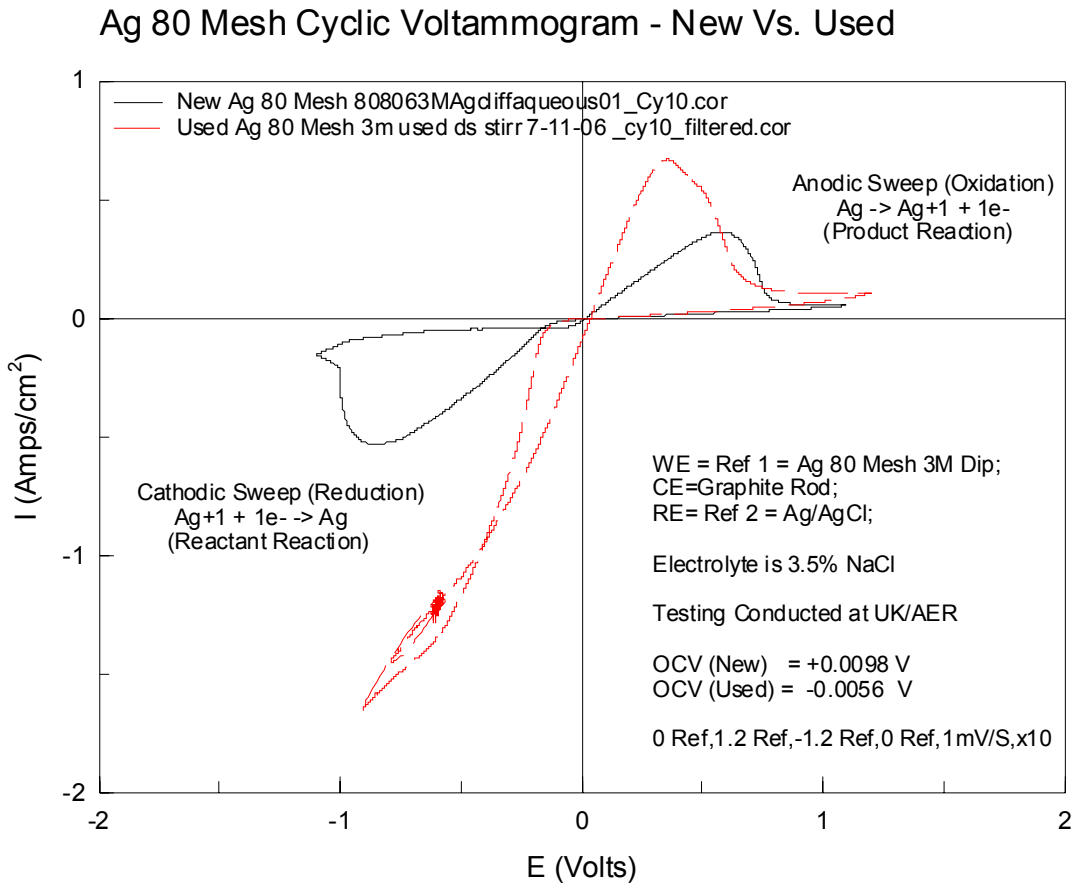

Figure 5.13 New/Used 80 Mesh Electrode CV Test Results

5.2.4 Pourbaix Diagram Discussion

The Pourbaix diagram distinguishes regions of active corrosion, passivity, and immunity in terms of pH, abscissa, and RedOx potential, ordinate. Figure 5.14 is a Ag Pourbaix diagram at 25°C in chloride solution at 1M concentration Cl^- , where (a) and (b) correspond to RedOx potentials determined by H and O saturation at standard temperature and pressure (STP)[24].

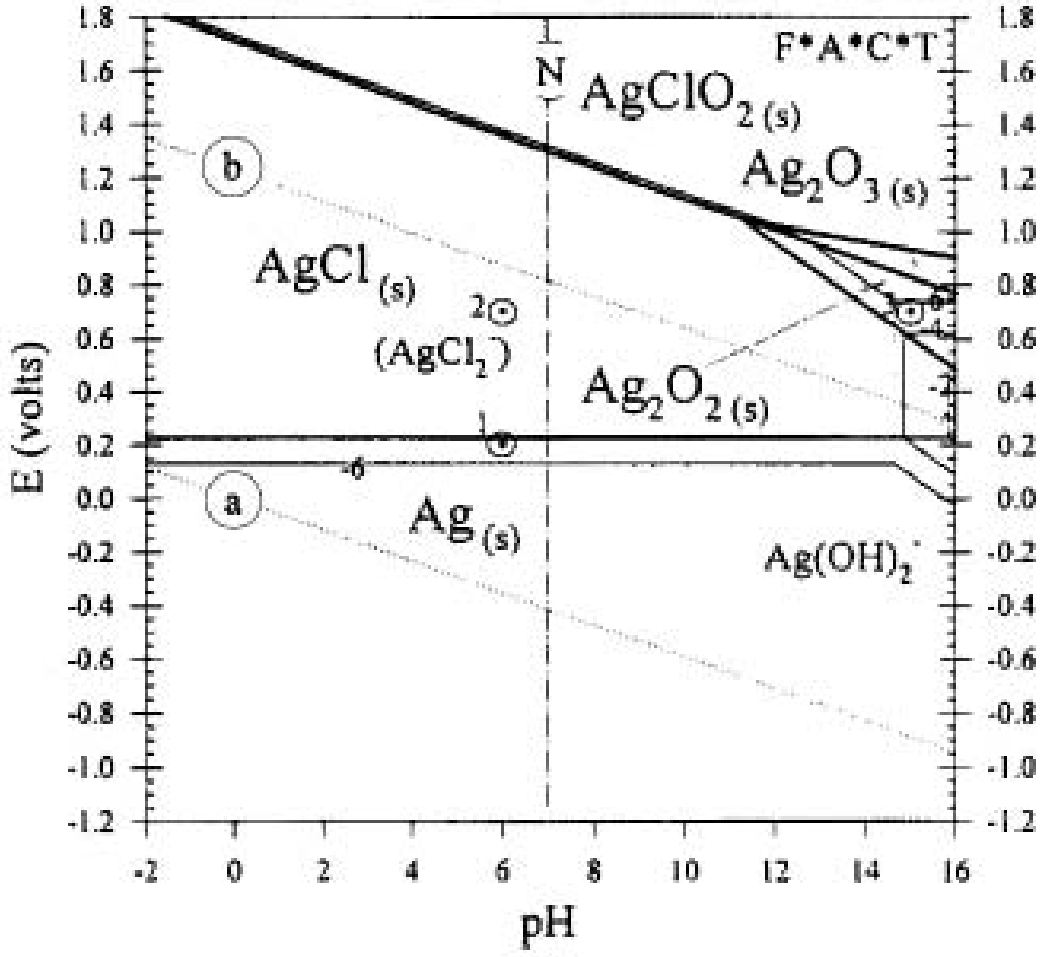

Figure 5.14 Ag Pourbaix Diagram at 25°C in Chloride Solution

Room temperature performance cell test results of pH and loaded cell potential, E, revealed pH ranges of 6.5 to 9.0 and E ranges of 10 to 20 mV DC. Figure 5.14 shows that at these values reveal that Ag may become an ionic species ($Ag \leftrightarrow Ag^{+} + e^{-}$), or will remains in its metallic form ($Ag \rightarrow Ag$) as a degenerate form. This is supported by SEM/X-Ray electrode analysis confirming primarily the presence of Ag alone in both new and used electrodes. All evidence supports the hypothesis that Ag is in equilibrium with its own ions Ag^{+} with the Cathodic/Anodic reactions occurring at the same rate in each cell side.

5.2.5 Electrode Summary

Analysis of electrochemical, physical, and performance based testing of the Ag mesh electrode confirmed that corrosion effects were found not to be a contributor to the overall cell potential and:

1) Functioned simply as charge collectors,
2) Confirmed electrode material selection, design, and ruggedness for subsequent field testing,
3) Allowed for the sole evaluation of the Bi-Polar membrane performance in a membrane based seawater concentration cell.

5.3 Bi-Polar Membrane Discussion

5.3.1 Membrane Details

Bi-Polar membranes from two manufactures were used in the testing effort. Details specific to each membrane are provided as follows:

1) Membranes International Inc., USA (MII BPM-9000):
    1. Primarily an industrial grade membrane used in the metal plating industry,
    2. Test cell dimensions: 4 inches by 4 inches, 2.75 by 2.75 in solution contact,
    3. Polymer structure – Gel polystyrene cross linked with divinylbenzene,
    4. Thick, stiff, “fabric-like appearance”,
    5. Shipped dry in “open” container,
    6. CEM: surface rough and dark color, Functional Group – Sulphonic Acid,
    7. AEM: Surface rough and light color, Functional Group – Quaternary Ammonium,
    8. Selected test cell measured and vendor provided sample properties:
        a. Dry Weight = 12.0532 grams
        b. Wet Weight = 13.7901 grams
        c. Water Uptake = 14.4%
        d. Thickness (dry) = 0.955 mm (0.0376 inches)
        e. Thickness (wet) = 1.082 mm (0.0426 inches)
        f. Electrical Resistance (Ohm) <1 (EIS Measured)

A used MII Bi-Polar membrane, CEM and AEM side, presented in Figures 5.15 and 5.16.

Figure 5.15 Used MII BPM-9000 Bi-Polar Membrane, CEM Side

Figure 5.16 Used MII BPM-9000 Bi-Polar Membrane, AEM Side

2) Fumatech, Germany (Fumasep® FBM):

    1. Primarily used in the water purification industry,

    2. Test cell dimensions: 4 inches by 4 inches, 2.75 by 2.75 in solution contact,

3. Polymer structure – (Kraton, PPO [poly(phenyleneoxide)]) cross linked with PEEK [Poly(etheretherketone)],
4. Thin, flexible, “sandwich wrap like appearance”,
5. Shipped in sealed container surrounded by 1 M NaCl solution,
6. CEM: surface smooth and shinny, Functional Group – Sulphonic Acid,
7. AEM: surface not slippery and opaque, Functional Group – Amines,
8. Selected test cell measured and vendor provided sample properties:
    a. Dry Weight = 1.7963 grams
    b. Wet Weight = 2.0705 grams
    c. Water Uptake = 15.3%
    d. Thickness (dry) = 0.189 mm (0.0074 inches)
    e. Thickness (wet) = 0.201 mm (0.0079 inches)
    f. Electrical Resistance < 3 Ohm

Used Fumasep® FBM membrane, CEM/AEM side, presented in Figures 5.17 and 5.18.

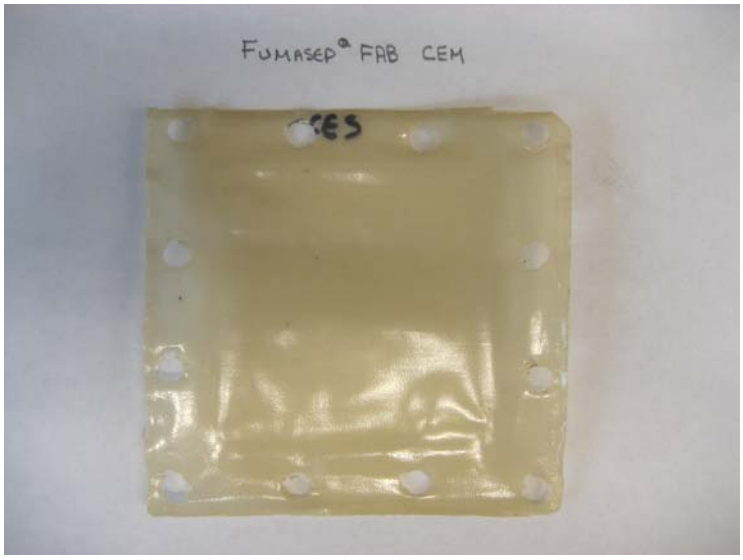

Figure 5.17 Used Fumasep® FBM Bi-Polar Membrane, CEM Side

Figure 5.18 Used Fumasep® FBM Bi-Polar Membrane, AEM Side

5.3.2 SEM Test Results and Summary

SEM images of both new and used MII BPM-9000 and Fumasep® FBM Bi-Polar membranes were made, see Figures 5.19 to 5.26.

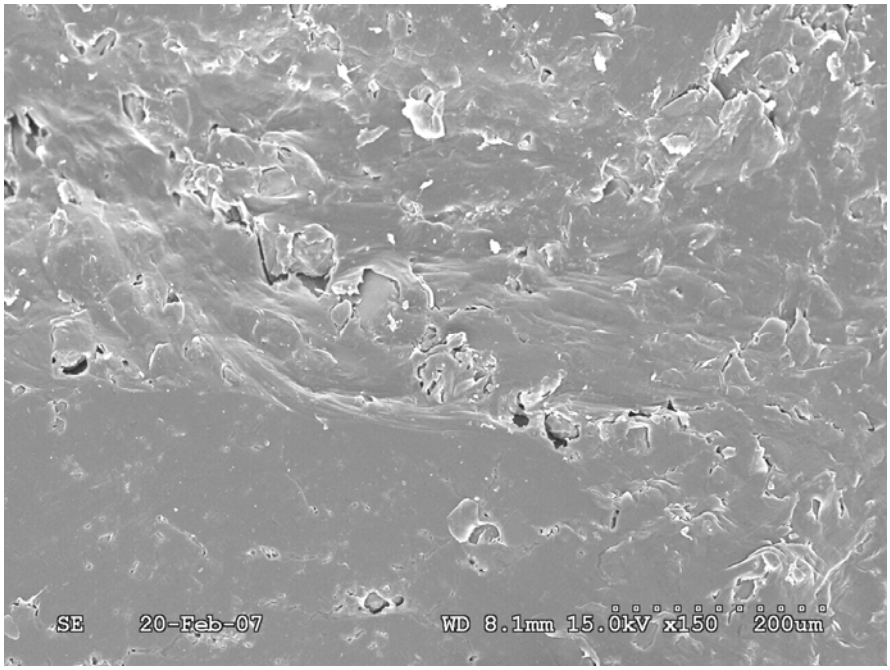

Figure 5.19 New MII BPM-9000 SEM Image, CEM Side

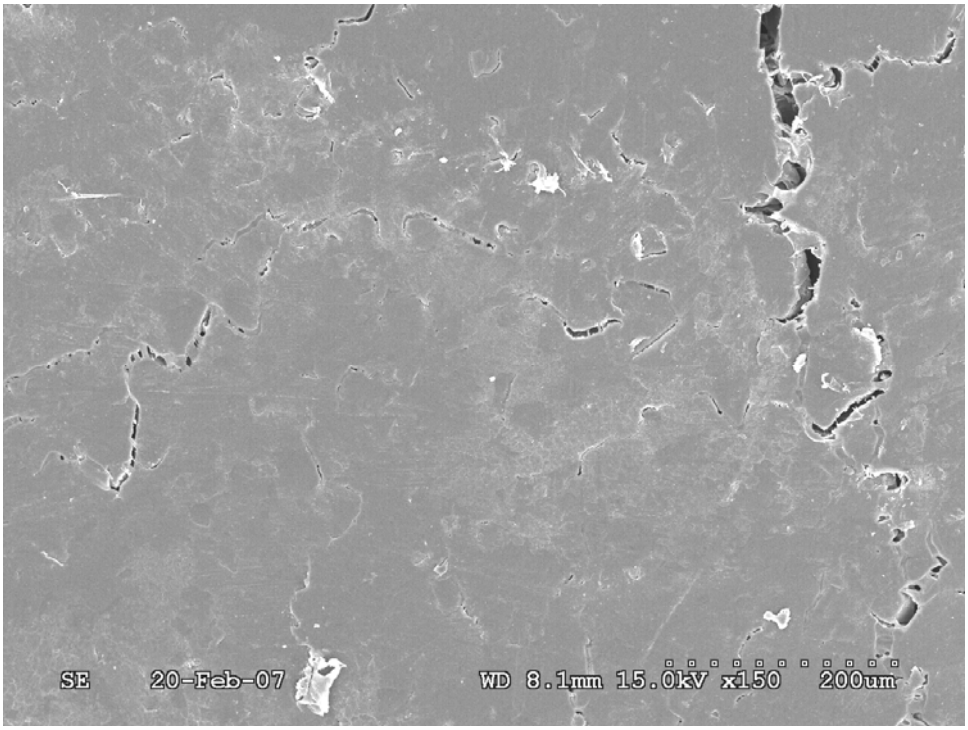

Figure 5.20 New MII BPM-9000 SEM Image, AEM Side

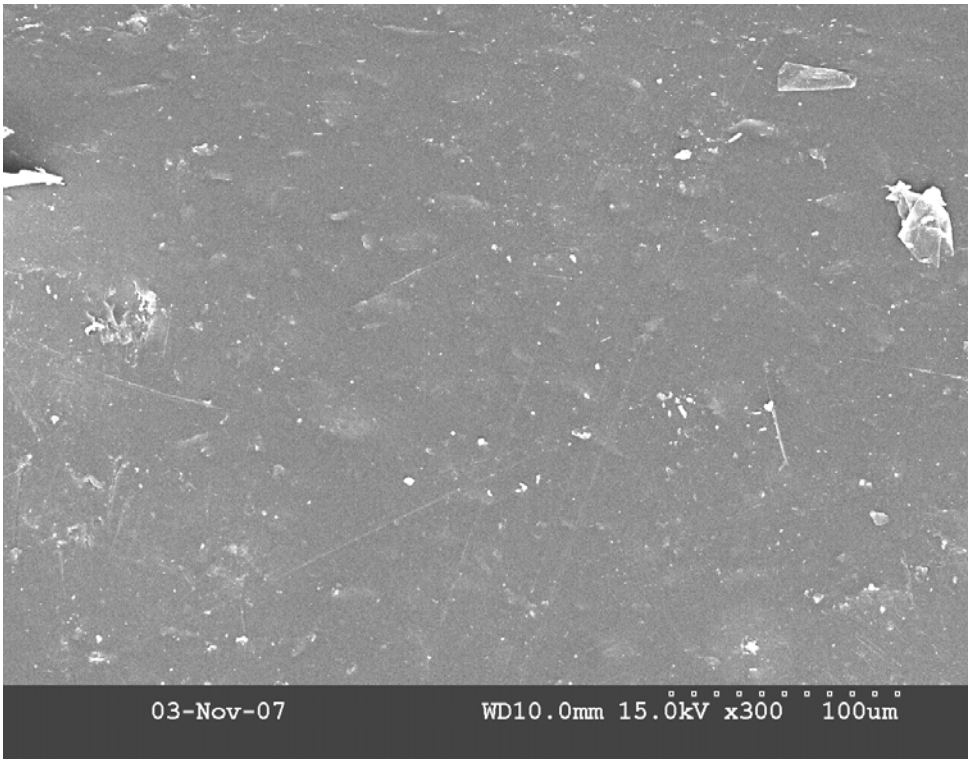

Figure 5.21 New Fumasep® FBM SEM Image, CEM Side

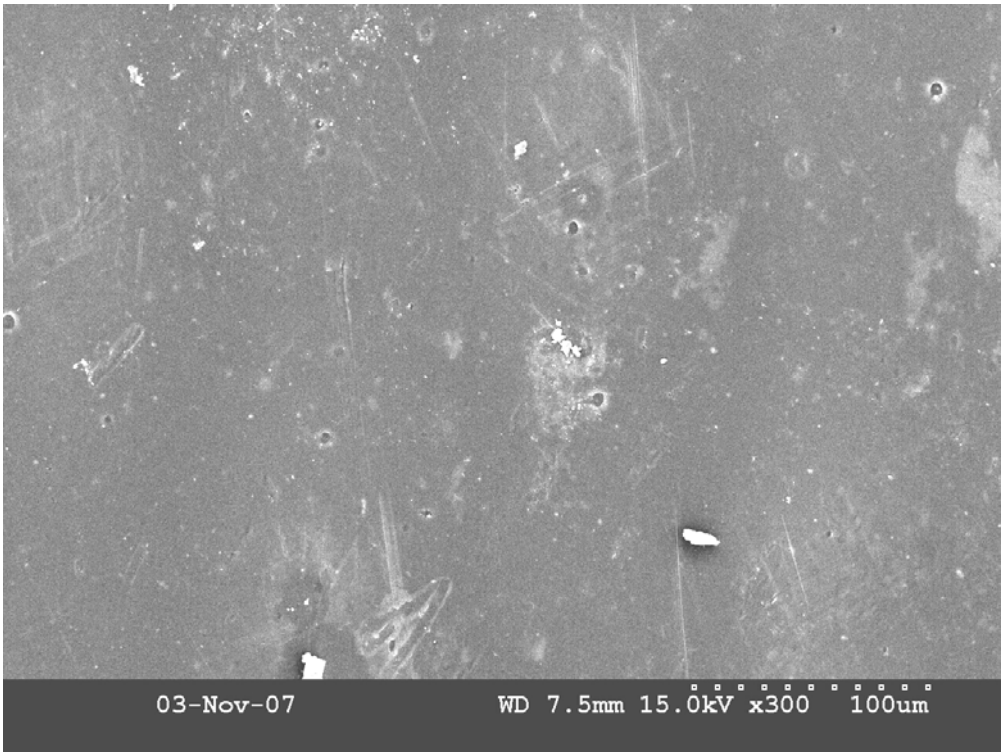

Figure 5.22 New Fumasep® FBM SEM Image, AEM Side

Figure 5.23 Used MII BPM-9000 SEM Image, CEM Side

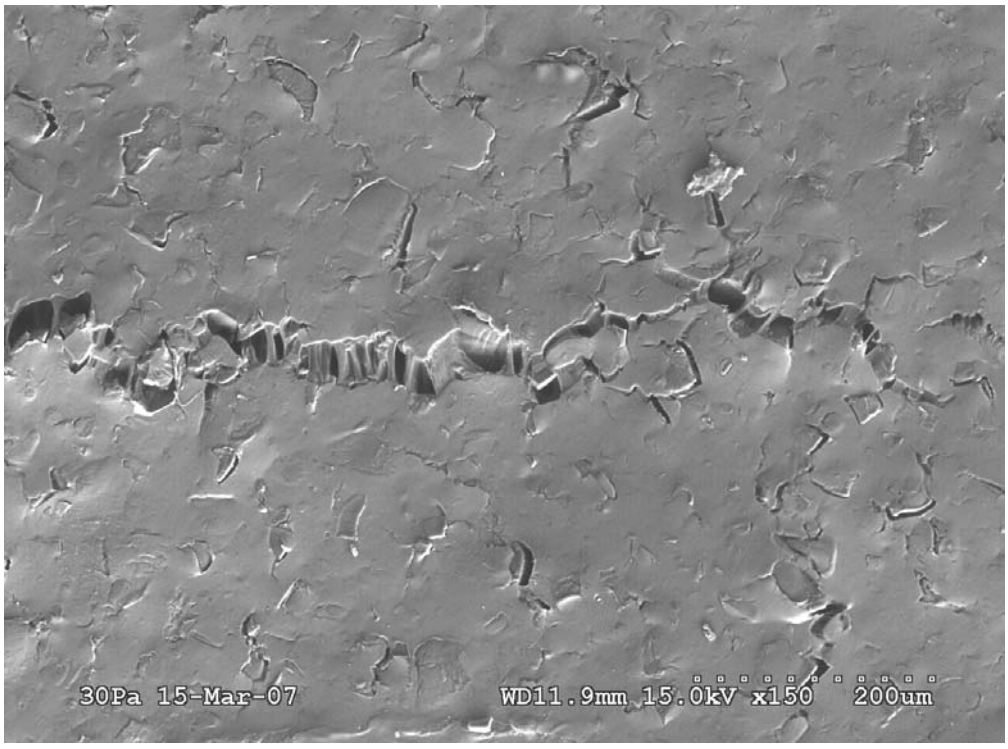

Figure 5.24 Used MII BPM-9000 SEM Image, AEM Side

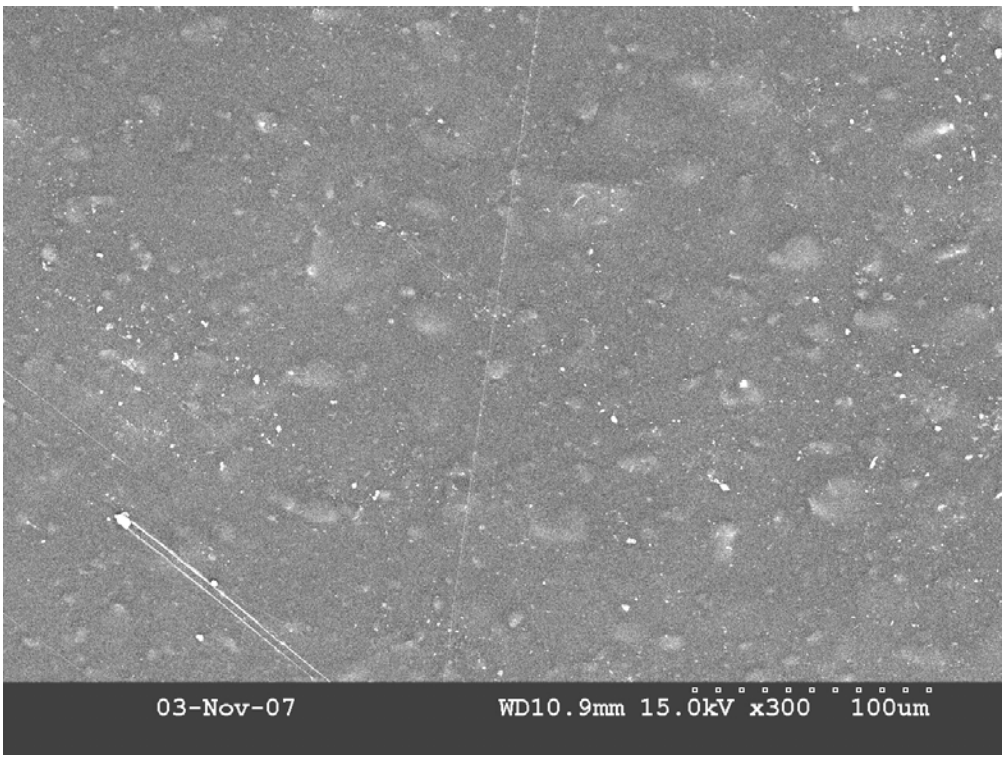

Figure 5.25 Used Fumasep® FBM SEM Image, CEM Side

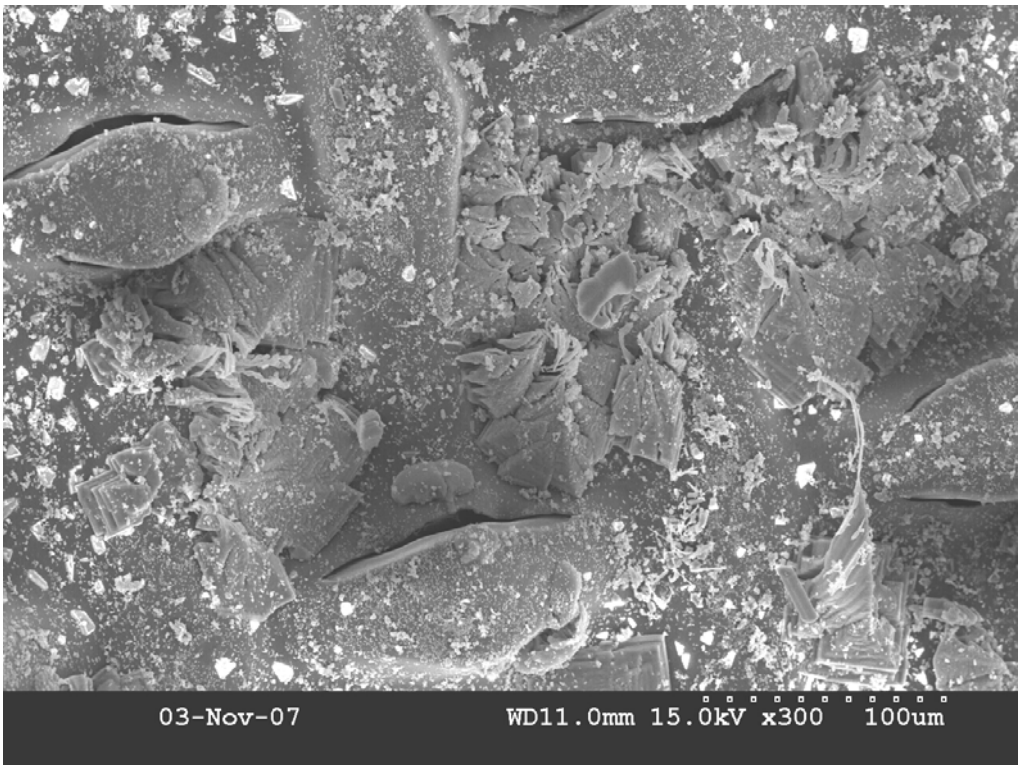

Figure 5.26 Used Fumasep® FBM SEM Image, AEM Side

Analysis of SEM images revealed:

1) The presence of many small holes distributed unevenly on the membrane surface,
2) The size of the membrane hole is sometimes much smaller than the distance between discrete holes and sometimes much larger than the distance between holes connected together in trench like lines,
3) That additional “openings” and “bumps” were present in the “USED” CEM/AEM membrane surfaces than were present when imaged new.

5.3.3 Membrane Summary

1) MII BPM-9000 and Fumasep® FPM Bi-Polar membranes were selected for testing because even though both were Bi-Polar membranes, they differed in composition, weight, stiffness, thickness, end application use, and cost.
2) Analysis of test data, however, revealed similar performance and water take up properties with results from DoE modeling showing no membrane manufacturer/end use related main effect interaction.
3) Based on the above findings:

    1. The small holes in these charged membranes could be acting in a voltammetric behavior on a microelectrode or ultra microelectrode scale[21].
    2. Combined membrane swelling and linkage of the "openings" present in used CEM and AEM membranes aided by the oppositely charged EDL can account for the measured Cl^- co-ion/counter-ion migration across the Bi-Polar membrane from concentrated to dilute sides of the functioning Bi-Polar concentration cell.

5.4. Electrochemical Impedance Spectroscopy Discussion

An excellent primer into the basis of EIS can be found in an application note entitled "Basics of Electrochemical Impedance Spectroscopy" by Gamry Instruments[25]. A brief EIS summary is included herein.

Ohm's Law applies to electrical circuits and states that the current through a conductor between two points is directly proportional to the potential difference (i.e., voltage drop or voltage) across the two points, and inversely proportional to the resistance between them. The mathematical equation that describes this relationship is:

$$E = IR$$

Where E is the potential difference in volts, I is the current in amperes, and R is a circuit parameter called the resistance (measured in ohms, also equivalent to volts per ampere).

Electrical resistance is the ability of a circuit element to resist the flow of electrical current. Ohm's Law can be rewritten in terms of resistance (Equation 5) as the ratio between voltage E and current I.

$$R = E/I \qquad \textit{Equation 5}$$

The simplest electrical circuit element is the resistor. An ideal resistor has the following simplifying but important properties:

1) Follows Ohm's Law at all current and voltage levels,
2) Its resistive value is independent of frequency,
3) AC current and voltage signals through a resistor are in phase with each other.

The real world contains additional circuit elements that exhibit much more complex behavior. These elements force the abandonment of the simple concept of resistance. In stead, the more general circuit parameter concept of electrical impedance or simply impedance is used. Electrical impedance extends the concept of resistance to alternating current (AC) circuits, describing not only the relative amplitudes of the voltage and current, but also the relative phases. Like resistance, impedance is a measure of the ability of a circuit to resist the flow of a sinusoidal AC electrical current. Unlike resistance, impedance is not limited by the simplifying properties listed above.

The mathematical representations of individual circuit elements can be converted into phasor notation, and then the circuit can be solved using phasors. In phasor notation, resistance, capacitance, and inductance can be combined together into a single term called "impedance" and like resistance, is measured in units of Ohms. The phasor used for impedance is "Z" and Ohm's law for phasors becomes:

$$E = IZ$$

and it's important to acknowledge that Ohm's law holds true for both the phasor domain as well as the time domain.

As mentioned, resistors do not affect the voltage or current, only the magnitude. Therefore, the impedance of a resistor with resistance R in phasor notation is:

$$Z = R \angle 0°$$

Capacitors and Inductor circuit elements do, however, affect the voltage or current. A capacitor with a capacitance C has an impedance value of:

$$Z = 1/\omega C\angle -\pi/2 \text{ or, in terms of degrees as, } Z = 1/\omega C\angle -90°$$

Illustrating that the current leads the voltage by 90°. Conversely, an inductor with an inductance L has an impedance value of:

$$Z = \omega L\angle \pi/2 \text{ or, in terms of degrees as, } Z = \omega L\angle 90°$$

Illustrating that the current lags the voltage by 90°.

Electrochemical impedance is measured by applying an AC potential to an electrochemical cell and measuring the current through the cell. Assuming a sinusoidal excitation is applied to a linear system, the response will be an AC current signal with the same frequency. This current signal can be analyzed as a sum of sinusoidal functions, a Fourier series.

Electrochemical impedance is normally measured using a small excitation signal (in this case 10 mV) so the cell's response is pseudo-liner. In a linear (or pseudo-linear system), the current response to a sinusoidal potential will be a sinusoid at the same frequency but shifted in phase (ϕ) as shown in Figure 5.27.

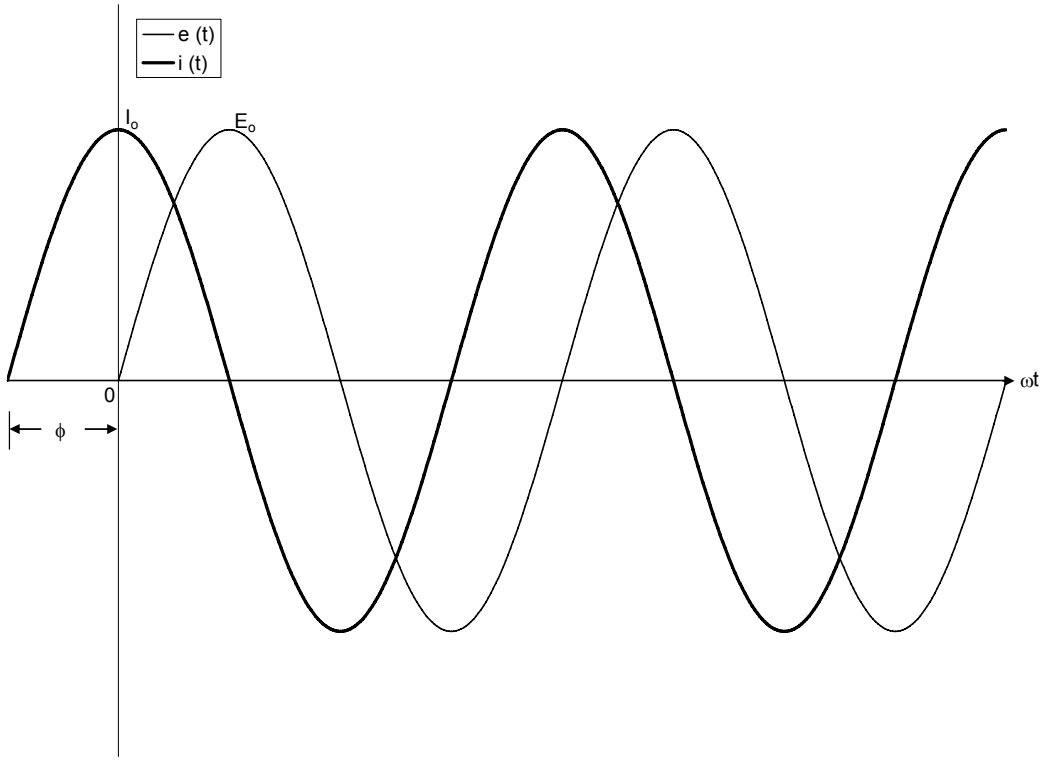

Figure 5.27 Sinusoidal Current Response in a Linear System

The excitation signal, e(t), expressed as a function of time, has the form:

$$e(t) = E_o \sin(\omega t + 0)$$

Where E_o is the amplitude of the signal, and ω is the angular frequency in radians/sec given by:

$$\omega = 2\pi f$$

Where *f* is the frequency in cycles per second (Hz). The excitation signal can also be expressed in phasor notation as:

$$E = E_o \angle 0°$$

In a linear system, the time domain response signal, i(t) is shifted in phase (ϕ) and has a peak amplitude, I_o.

$$i(t) = I_o \sin(\omega t + \phi)$$

Similarly, the response signal can also be expressed in phasor notation as:

$$I = I_o \angle \phi$$

By Ohm's law, the impedance of the system is written in Equation 6 as:

$$Z(\omega) = E_o \angle 0 / I_o \angle \phi = |Z_o| \angle -\phi \qquad \textit{Equation 6}$$

The impedance is therefore expressed in terms of a magnitude, Z_o, and a phase shift ϕ. Equation 6 has both real and imaginary parts. Plotting the real part on the X-axis and the imaginary part on the Y-axis, produces a "Nyquist Plot" as presented in Figure 5.28. On the Nyquist Plot the impedance can be represented as a vector (arrow) of length |Z|. The angle between this vector and the X-axis is the phase angle ϕ (= arg Z)). The semi-circle is characteristic of a single "time constant" system.

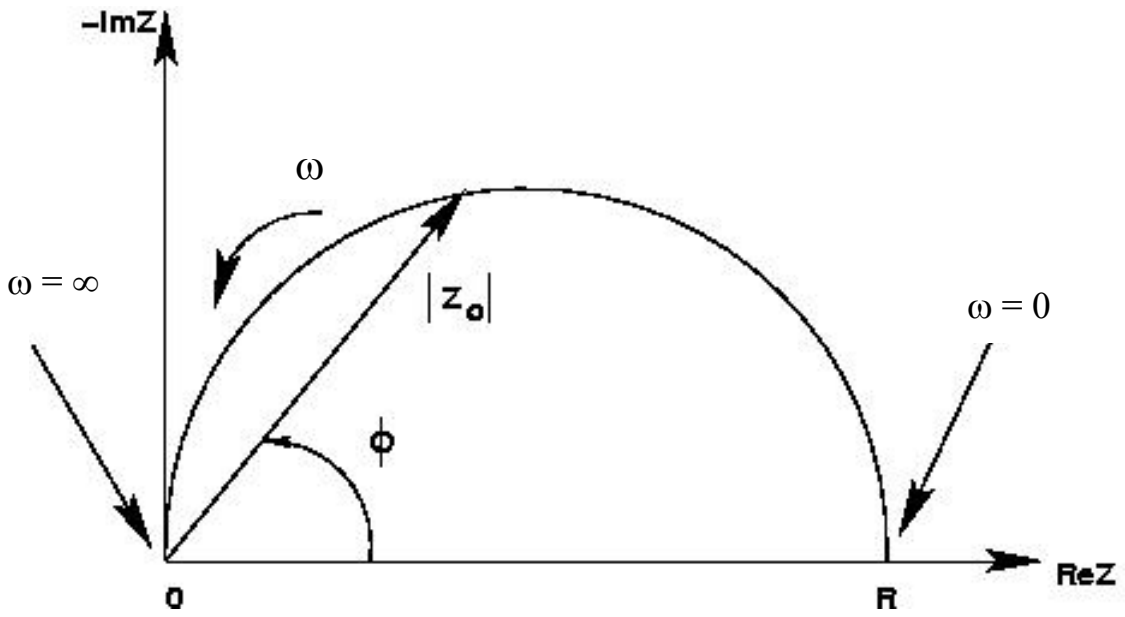

Figure 5.28 Nyquist Plot with Impedance Vector

The Nyquist Plot in Figure 5.28 results from the electrical circuit of Figure 5.29. Another popular method is the Bode Plot. The impedance is plotted with log frequency on the X-axis and the impedance and the phase-shift on the Y-axis. The Bode Plot for the electric circuit of Figure 5.29 is shown in Figure 5.30. Unlike the Nyquist Plot, the Bode Plot does show the frequency information.

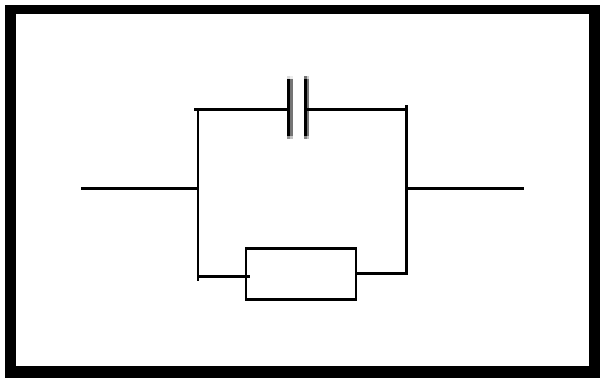

Figure 5.29 Simple Equivalent Circuit with One Time Constant

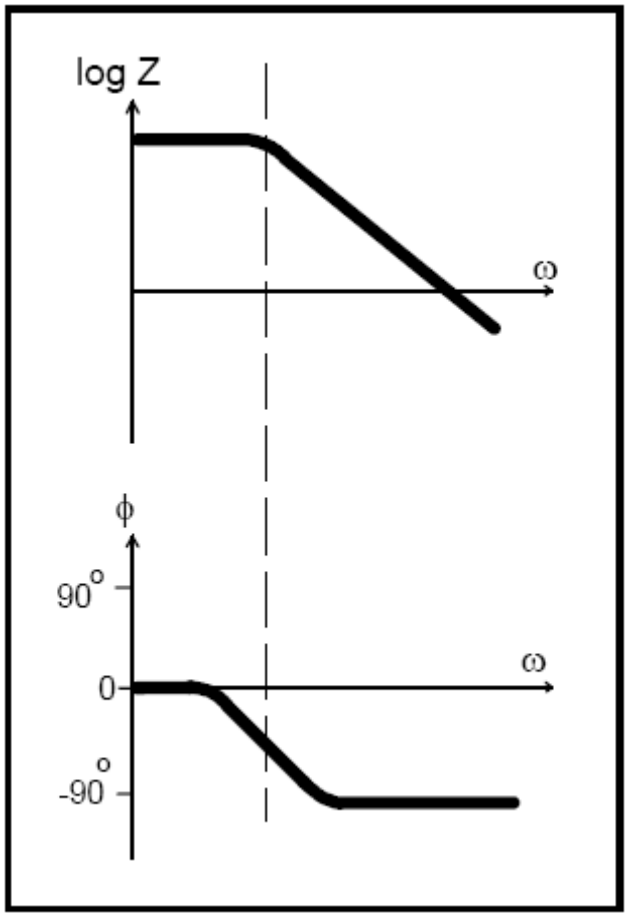

Figure 5.30 Bode Plot with One Time Constant

5.4.1 Equivalent Circuit Modeling Discussion

EIS data is commonly analyzed by fitting it to an equivalent electrical circuit model. To be useful, the elements in the model should have a basis in the physical electrochemistry of the system. As an example, most models contain a resistor that models the cell's solution resistance. Solartron's ZView2 software package was used for both EIS Impedance and Equivalent Circuit Modeling (ECM) analysis and display. EIS

determined values of the 3.6M//0.45M Solution Resistance (Rs) were approximately equal to: 0.33 Ohms for 3.6M Cl^- and 1.41 Ohms for 0.45M Cl^- solutions and 0.69 Ohms for the MII membrane resistance (R_m).

The Bi-Polar membrane concentration cell was closely modeled as a Randles' Cell in parallel with an external load as presented in Table 5.1 and Figure 5.31. The exception here being that the Randles Cell ideal capacitor, in parallel with the system Polarization Resistance (Rp), is replaced by a Constant Phase Element (CPE). This was done because "Double Layer Capacitors" in real electrochemical cells are sometimes modeled as a CPE rather than single capacitive elements.

The impedance of the CPE can be expressed as:

$$Z = (1 / Y_o)(j\omega)^{-\alpha}$$

Where,

$Y_o = C$ = the Capacitance and,

α = An exponent that equals 1 for an ideal capacitor and <1 for a CPE

While several theories (surface roughness, "leaky capacitor", non-uniform current distribution, etc.) have been proposed to account for the non-ideal behavior of the double layer, α is treated here as an empirical constant with no physical basis until additional research is conducted and a more generally accepted theory put forward.

Table 5.1 ECM - 1:10 MII RT OCV Data

Element	Freedom	Value
Rext	Fixed (X)	1E09
2Rs + Rm	Fixed (X)	2.901
CPE-T	Fixed (X)	0.0031
CPE-P	Fixed (X)	0.764
Rp	Fixed (X)	2550

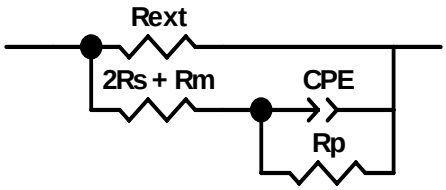

Figure 5.31 ECM - 1:10 MII RT OCV

The Nyquist Plot in Figure 5.32 results from the electrical circuit of Figure 5.31. Examination of Figure 5.32 shows a reasonable good fit between OCV modeled and measured results with the exception being in the extreme low frequency region which is attributed to local environmental noise contamination. Also evident is the depressed semi-circle, characteristic of a parallel RC circuit element.

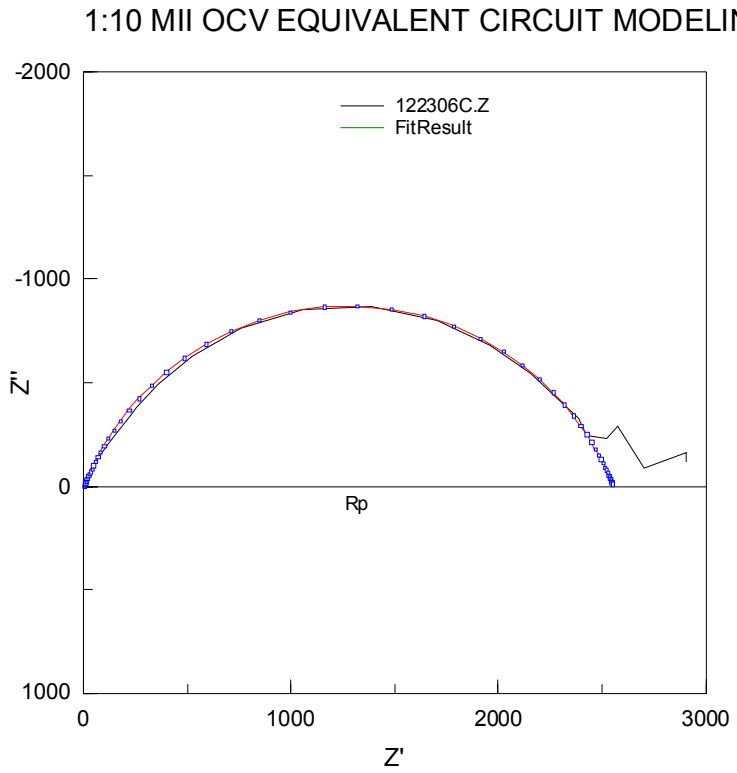

Figure 5.32 Nyquist Plot - 1:10 MII RT OCV - Measured vs. Modeled

5.4.2 ECM Model Result Under External Electrical Loading Discussion

ECM model result comparison analysis was conducted using the same developed OCV model with the exception that R_{ext} was changed from near infinity (1E09) Ohms to R_{ext} = 500 Ohms as presented in Table 5.2 and Figure 5.33. No high frequency semi-circle was seen in the Nyquist plot, shown in Figure 5.34, nor present was a step in the intermediate frequency area in the Bode diagram, see Figure 5.35, therefore, the Interfacial Capacitance is large enough to compare to the systems high Rp value (e.g. metals with very low corrosion rates[26]) at frequencies low enough that the overall cell

impedance ($Z^{|}$) ≈ Rct (Charge Resistance). Further examination of Figure 5.35 reveals a (-) phase angle which is indicative of a capacitive impedance network.

Table 5.2 ECM - 1:10 MII RT 500 Ohm Ext Load Data

Element	Freedom	Value
Rext	Free (+)	500
2Rs + Rm	Fixed (X)	2.901
CPE-T	Fixed (X)	0.0031
CPE-P	Fixed (X)	0.764
Rp	Fixed (X)	2550

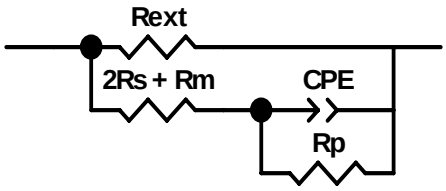

Figure 5.33 ECM - 1:10 MII RT 500 Ohm Ext Load

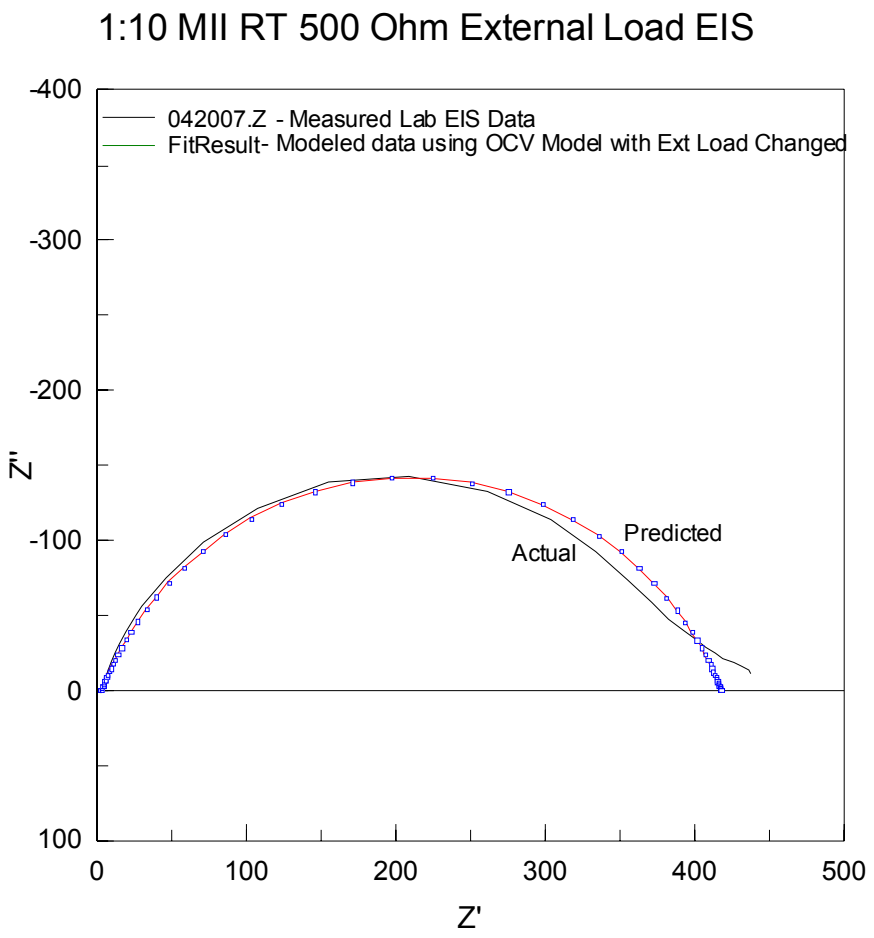

Figure 5.34 Nyquist Plot - 1:10 MII RT 500 Ohm Ext Load - Measured vs. Modeled

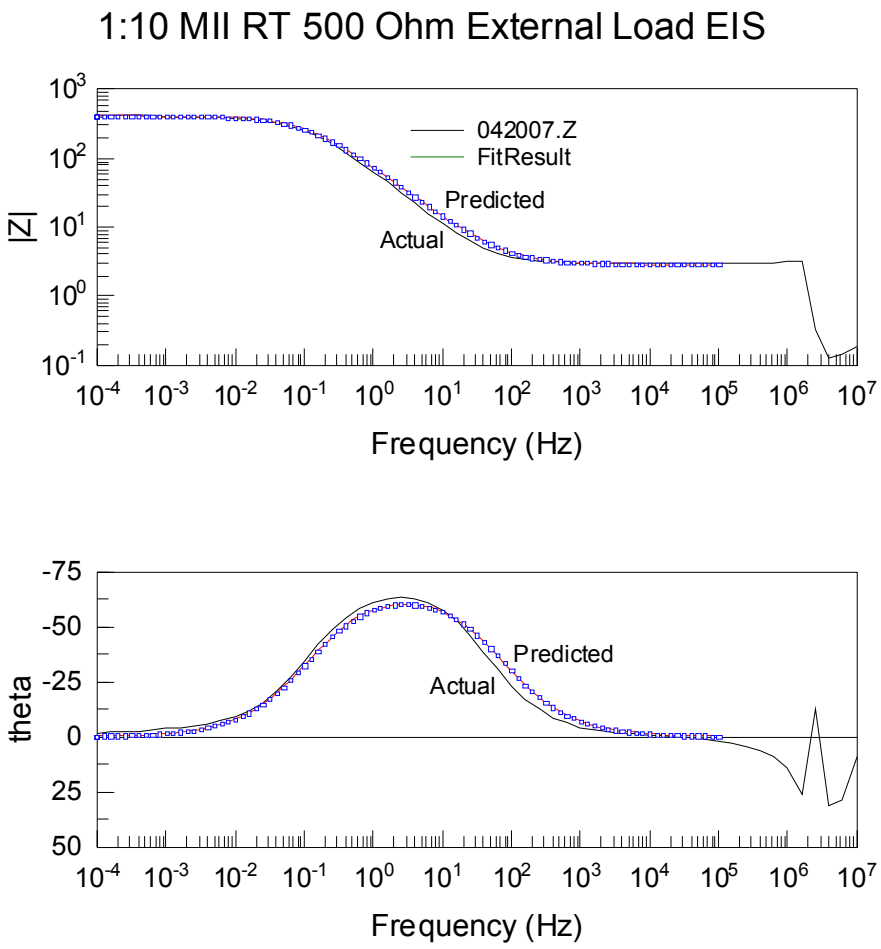

Figure 5.35 Bode Plot - 1:10 MII RT 500 Ohm Ext Load - Measured vs. Modeled

Diffusion can create impedance called Warburg impedance. On a Nyquist plot, the Warburg impedance appears as a diagonal line with a slope of 45° at very low frequencies. On a bode plot, the Warburg impedance exhibits a phase shift of 45°. No evidence of this low frequency diffusion control was evident in either the Nyquist or Bode plots. This supports the proposed model as primarily a parallel combination of CPE Interfacial capacitance and polarization resistance. This in conjunction with the corrosion evidence supports belief that Ag is in equilibrium with its own ions Ag^{+} with

the Cathodic/Anodic reactions occurring at the same rate in each cell side, as previously discussed in Section 5.2.4.

Whenever the potential of an electrode is forced away from its value at open circuit it is referred to as "polarizing" the electrode. When an electrode is polarized, it can cause current to flow through electrochemical reactions at the electrode surface. The amount of current is controlled by the kinetics of the reactions and the diffusion of reactants both towards and away from the electrode. In this case, where RedOx reactions are occurring at the same rate in each cell side, a single kinetically-controlled electrochemical reaction at equilibrium occurs and charge is transferred. This charge transfer reaction has a certain speed depending upon the kind of reaction, the temperature, the concentration of the reaction products and the potential.

When the polarization depends only on the charge-transfer kinetics the Butler-Volmer equation can be used to estimate the value of R_{ct} at equilibrium as:

$$R_{ct} = RT/nFi_o \qquad \textit{Equation 7}$$

Using data presented later in Section 5.9, Table 5.3, a MII 80 Mesh 22°C (RT) performance test run under an external load of 500 Ohms resulted in an equilibrium voltage of nominally 15.5 mV. Remembering Ohm's Law, this results in a value of i_o (exchange current density) of nominally 3E-5 Amps. Back subbing into Equation 7 results in:

$$R_{ct} = [(8.314\ J\ K^{-1}\ mol^{-1} * 295K) / (1 * 96{,}500\ C\ mol^{-1} * 3E\text{-}5A)] \sim 850\ Ohms$$

Which is approximately double the value of Z' shown in Figure 5.34. Although close in value it indicates the overall cell potential does not depend solely on the electrode charge-transfer kinetics. A likely contributor is the Donnan exclusion of the reaction products under the internally generated concentration gradient driving force (Section 2.8).

5.5 Bi-Polar Membrane Concentration Cell Electrical Loading Discussion

Cell loading measurements were made on numerous runs using both EIS techniques as well as direct DC monitoring of the cell output potential using a digital volt meter (DVM)/data logger/computer storage system. Representative plots of each are presented in the following sections.

5.5.1 Electrical Loading Comparison

Figure 5.36 presents a 5-day run consisting of both OCV and varying load conditions. Of particular importance revealed is the consistency and repeatability of conditions, starting at OCV (69 mV), with a 1K Ohm load (18.2 mV), then a 500 Ohm load (8.7 mV), then a 10 Ohm load (0.25 mV), followed back to OCV (68 mV) and then back to a 500 Ohm load (8.2 mV). This confirms a parallel external load connection with the cell, resulting in a halving of cell output with a halving of externally applied load. Revealing a fairly constant cell output current condition across the load conditions tested.

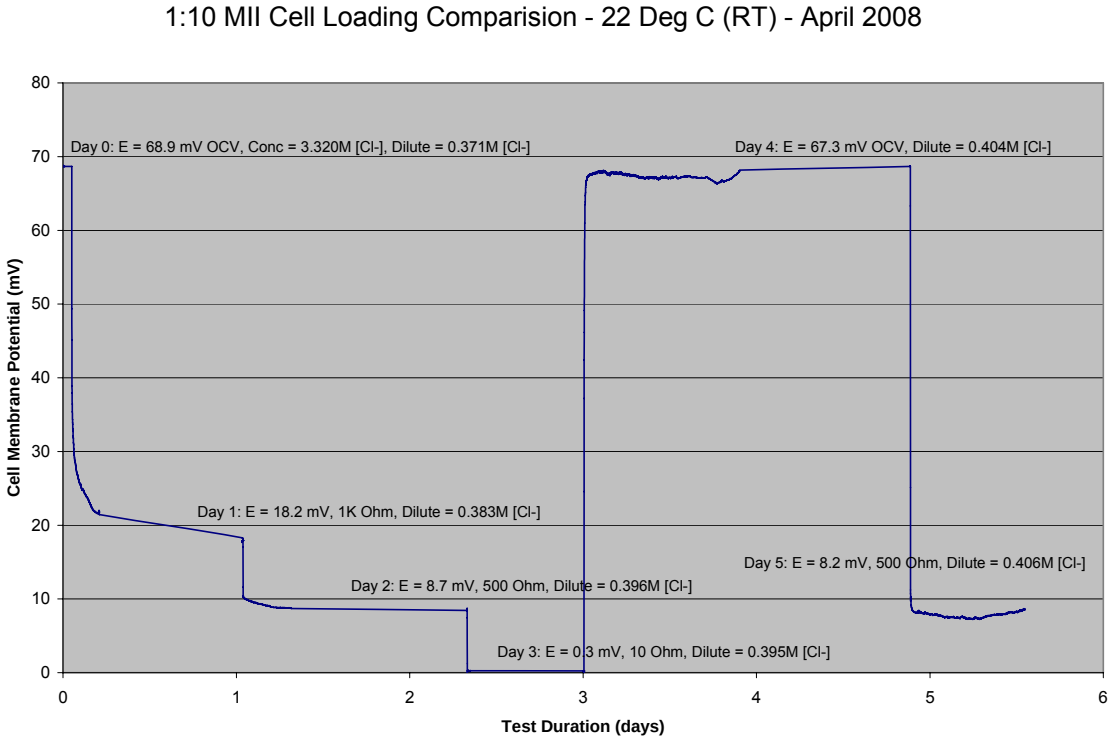

Figure 5.36 1:10 MII RT Cell Loading Comparison

Agitation of the cell was performed at various times before and after this test and although variations did occur in the OCV condition, the affects were small (<5%) under load. With loaded equilibrium quickly reached once the agitation was removed.

5.5.2 EIS Comparison during Loading

Figure 5.37 presents various EIS test results for variations in concentration ratios and external loading values for a standard 80 Mesh MII test configuration run in the (+) membrane convention under solution pumping (nominally 430 ml/day). With the exception of OCV conditions, no applicable difference in measured cell impedance was noted with a 10 fold increase in concentration differences. While a doubling of the

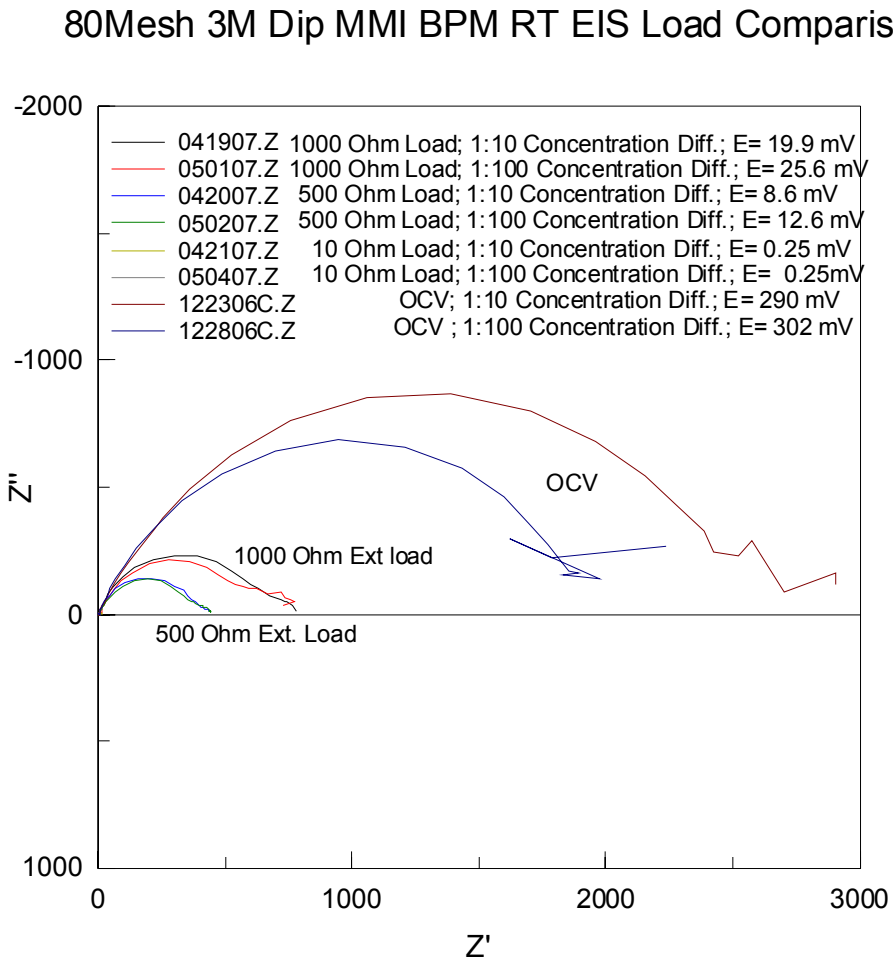

Figure 5.37 EIS Load Comparison Plot

applied external load results in an approximate doubling of the cell output membrane potential (parallel connected); a 10 fold increase in solution concentration does not produce a doubling of cell output as predicted by the Nernst Equation. Therefore, test results illustrate that the Bi-Polar membrane concentration cell operation under external loading can not be adequately described by the Nernst Equation[27].

5.6 Solution Pumping Speed Dependency on Cell Output Potential

The effects of pumping speed on cell performance were evaluated by examining the measured change in a loaded 80 mesh MII 1:10 room temperature cell operated under differing fluid pumping speeds. Figure 5.38 presents an impedance comparison plot showing variation from low to high speed, 0.0036 ml/sec (310 ml/day) to 0.0064 ml/sec (550 ml/day), respectively. Data analysis revealed a minimal change in overall cell impendence under a nominal 500 Ohm load and a resulting negligible 1 mV variation in output voltage.

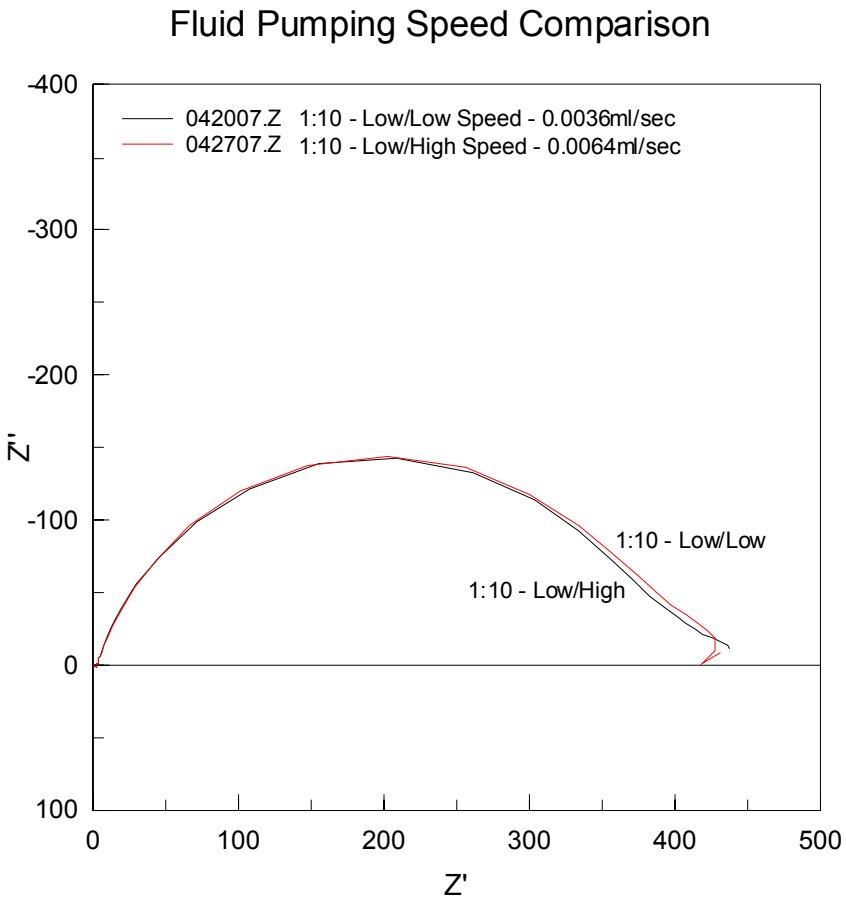

Figure 5.38 1:10 MII 80 Mesh Fluid Pumping Speed Comparison Test

Final system operation consisted of dual peristaltic pumps (one for each cell side), positioned over a reservoir of synthetic seawater of varying concentrations and operating at the same speed (nominally 430 ml/day). This set up was run in both a laboratory grade incubator/oven or refrigerator/freezer to obtain the temperature affects desired (Figure 5.2).

5.7 Bi-Polar Membrane Orientation Discussion

The difference in membrane output potential and how it may vary depending upon which Bi-Polar membrane side (CEM or AEM) is in contact with the concentrated and dilute solutions was investigated. Figure 5.39 presents an 8-day data plot of a room temperature measurement of 1:100 concentration cell membrane potential under the condition of a nominal 500 Ohm external load, 80 mesh electrodes, and a MII membrane. Close examination of Figure 5.39 reveals a significant difference in output membrane potential with membrane orientation as illustrated by the data plots and corresponding orientation layout schematics. Investigation reveals that for maximum potential output, the cell needs to operated in what is typically referred to as the (+) Bi-Polar membrane orientation, that being with the concentrated solution in contact with the Bi-Polar membrane AEM side and the Bi-Polar membrane CEM in contact with the dilute solution side. Also illustrated in the orientation layout schematics are the measured electrode polarities, which in the case of the preferred (+) orientation is the same as an electrolytic cell, discussed in Section 2.2.

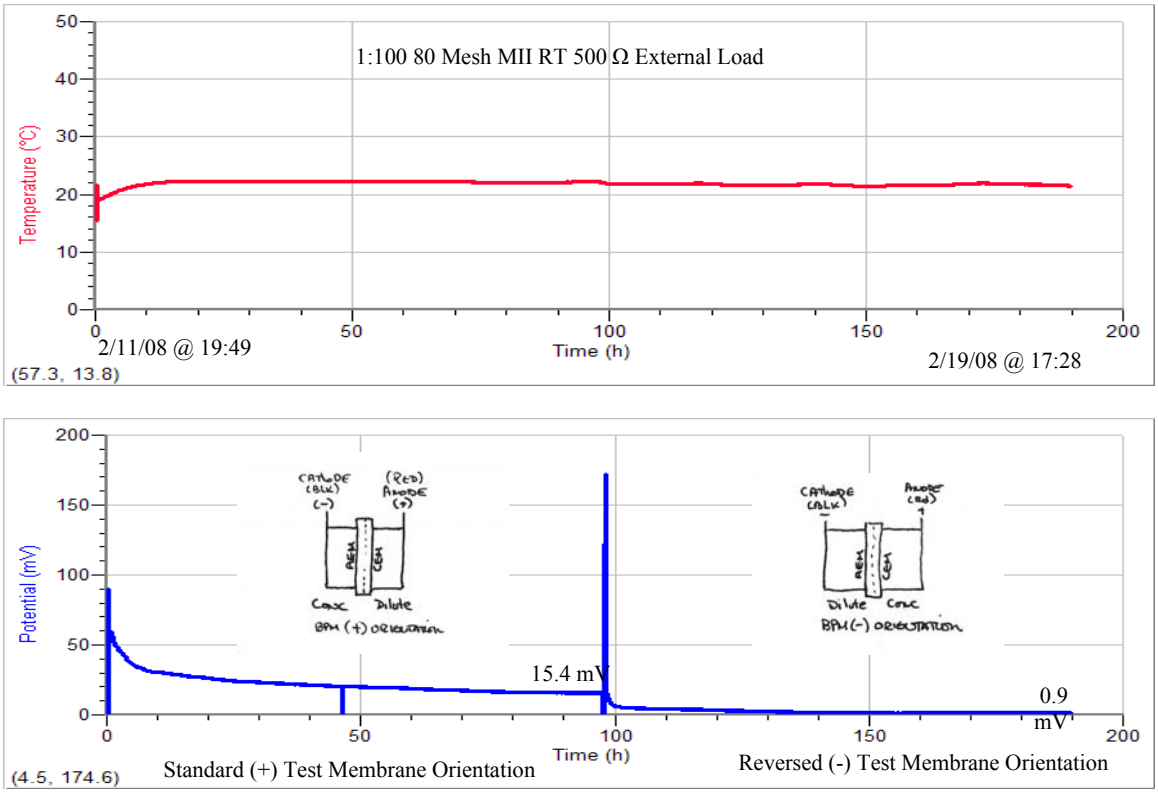

Figure 5.39 1:100 MII 80 Mesh Bi-Polar Membrane Orientation Test

5.8 Bi-Polar Membrane Concentration Cell Ion Migration and Osmotic Flow

Ion Migration and Osmotic Flow investigations were made on numerous runs. Visual evidence of Positive Anomalous Osmosis – confirming the migration of solvent, water, moving across the Bi-Polar membrane from the dilute side to the concentrated side – is presented in Figure 5.40. Figure 5.40 clearly shows an accumulation of solvent overflowing from the concentrated side of the cell in this standard (1:10 MII 80 Mesh) example of a room temperature, static (no pumping occurring), open cell configuration.

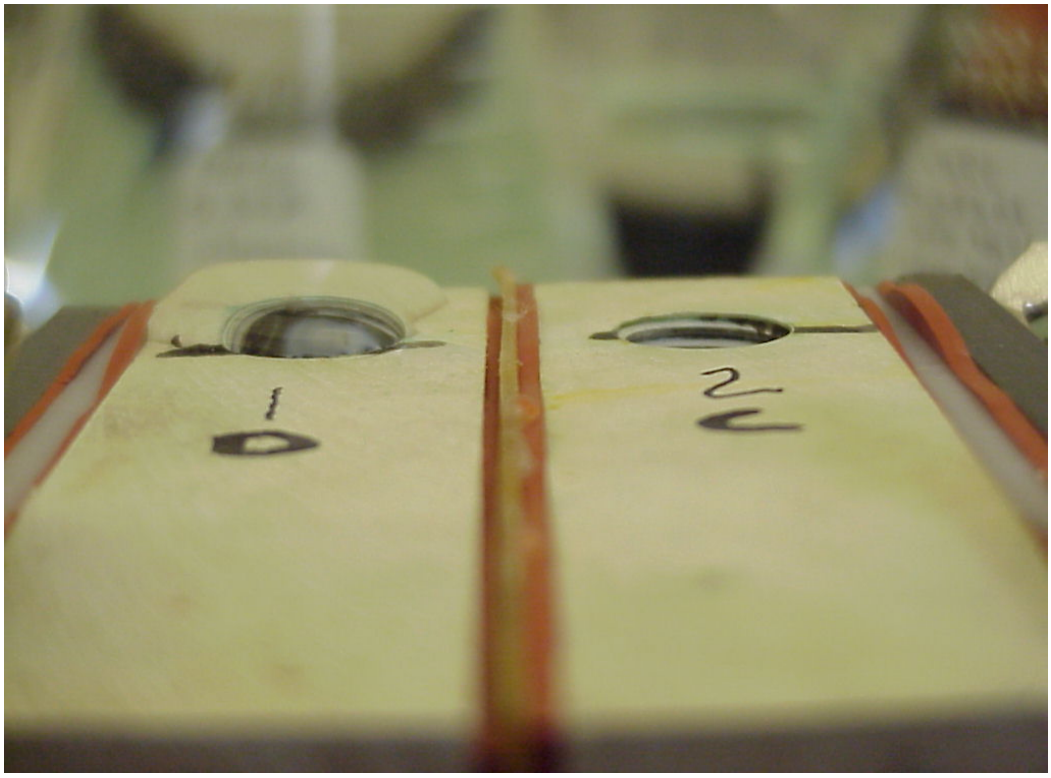

Figure 5.40 Evidence of Positive Anomalous Osmosis

Figure 5.41 presents a 6-day room temperature performance measurement of a 1:10 MII cell membrane output potential under OCV and varying external loading in the (+) Membrane Orientation. Close examination of this plot reveals very similar OCV pre- and post-loading values along with the previously shown halving of cell output corresponding to a halving of external load. Interesting here is that although the OCV values are similar, the loaded cell membrane potential values are about a half of that previously shown, for similar loading conditions. Illustrating a repeatable but variable output potential which will be discussed and quantified in detail in the following section, Section 5.9, DoE Modeling Discussion. This variation was, however, within the 95% Confidence Intervals (CI) computed and provided in the Section 5.9 results section.

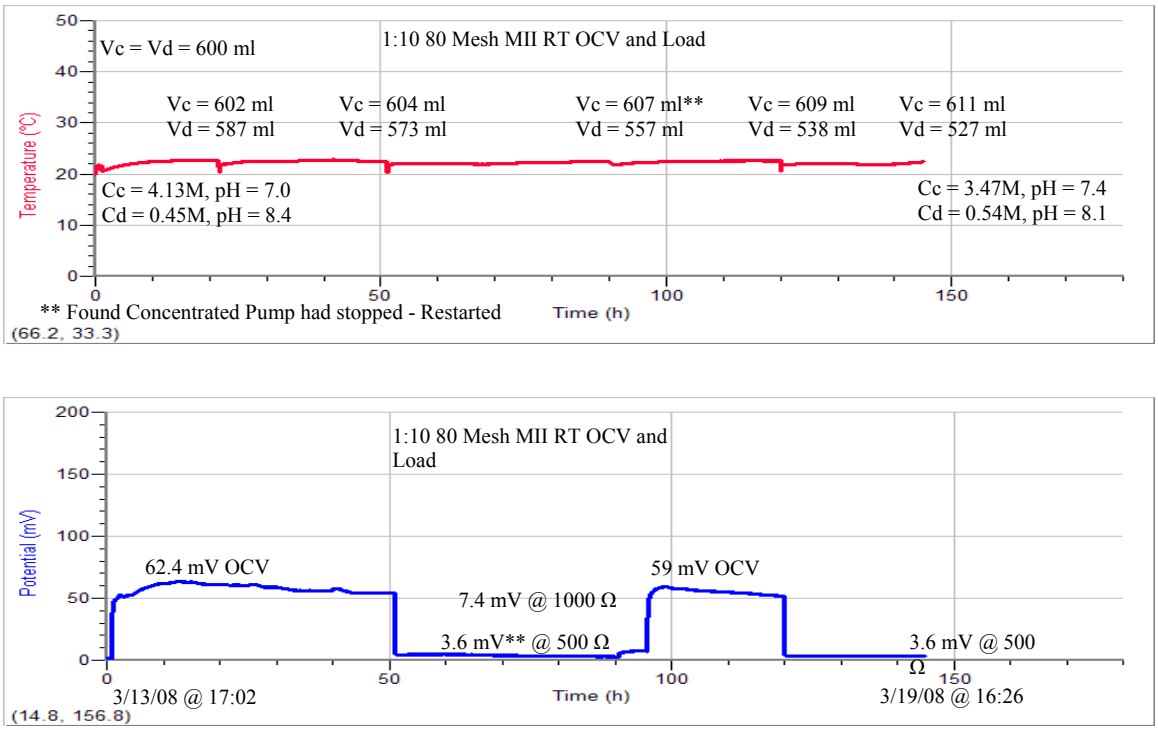

Figure 5.41 Ion Migration and Osmotic Flow Example

Revealed in Figure 5.41 is the measurement of the volume in the cell output beaker verses time for both the concentrated and dilute side. As shown, there is an overall increase in the concentrated side volume and a decrease in the dilute side volume with time, indicating a net transport of solvent (water) across the membrane from dilute to concentrated (Anomalous Positive Osmosis). Shown also are the results of numerous Cl^- titrations made during the test revealing a net decrease in Cl^- ions in the concentrated side and an increase in the dilute side.

Interesting that although small in amount, there was more loss in dilute volume than in concentrated volume gain. The concentrated side pump had stopped sometime

during the evening mid way in the test and could attribute as well as a slight cell leakage of the AEM side along with some solvent passage through the membrane with the Cl^- ions within their hydration shells. pH measurements made during this test run reveal an increase in the pH of the concentrated solution and a decrease in the pH of the dilute solution. Although the measured cell output potentials were far lower than the theoretical "water splitting" potential value of 0.828 (Section 2.6.2.1), it is still possible that the water passing through the AEM dissociates (splits) into equivalent amounts of H^+ and OH^- ions within the intermediate layer. These ions could then migrate with the H^+ ions permeating through the CEM side and the OH^- ions permeating the AEM side, affecting the pH as seen. Both these areas will be examined in more detail in follow-on research.

5.9 Design of Experiment Modeling Discussion

Because the Nernst Equation did not adequately predict the cell output performance under load, a DoE approach was implemented to determine a suitable equation defining the cell loaded output performance. An evaluation of pertinent factors that might affect cell membrane potential output performance was conducted and resulted in eleven (11) factor variables: electrode composition, electrode surface area, solution concentration, solution composition, solution flow rate, cell temperature, membrane type, membrane orientation, operating pressure, agitation, and external electrical loading. That's 2^{11} or 2048 runs with a single replicate. Screening experiments were performed to reduce this number down significantly by systematically examining each variable while keeping in mind the focus of this research effort – that being to investigate the membrane

potential of a seawater concentration cell and its suitability as a low power energy source for micro and nano devices, such as wireless communication devices.

With anticipated sea surface operation, the need to test at any pressures other than atmospheric was removed. Seawater solution composition variation was minimized through the use of synthetic seawater. Membrane orientation was examined separately and (+) orientation was used extensively through out the DoE test program. Solution flow rate was examined separately and found to be negligible at the anticipated flow rates. External loading effects on cell performance were examined and quantified separately and all DoE testing conducted with an external load of 500 Ohms present. Electrode composition variation issues were removed from contributing to the overall cell potential via careful material selection and the use of identical electrodes for both cell sides. Cell agitation was observed to have an affect on the cell potential in the OCV condition but the affect was negligible when an external electrical load was present. This effectively reduced the variable count down to four (4), however, because of the number of possible coupled interactions with just four, a fractional, factorial experimental design using SAS statistical DoE analysis package was used to determine the significant factors in the concentration cell output potential voltage (E1) in terms of:

1) Electrode surface area (ESA),
2) Bi-Polar membrane end use type (MEM),
3) Synthetic seawater solution concentration (CONC),
4) Cell operating temperature (TEMP).

5.9.1 Test Set-up Discussion

A 2^{4-1} fractional, factorial design was chosen for this purpose. Using a 2^{4-1} design, four variables were studied at two levels by performing eight experiments ($2^{4-1} = 8$). The response (E1) is the magnitude of the concentration cell output voltage in mVDC operated in the (+) membrane orientation and under an external electrical load of 500 Ohms. The design of experiment matrix (Table 5.3) shows the measured response along with the two levels of the variables coded such that a minus one (-1) represents the low level and a plus one (+1) represents the high level. These variables and coded levels were chosen based on previous experiments and practical considerations anticipated to be encountered in the field for an operational seawater concentration cell.

Table 5.3 Engineering Design Test Results with 500 Ohm External Loading

Run	ESA	MEM	CONC	TEMP	Date	Temp °C	Cell Voltage (mV DC)
1	80 (-1)	FUM (-1)	1:100 (-1)	L (-1)	10/29/07	4.6	3.4
2	40 (1)	FUM (-1)	1:100 (-1)	H (1)	11/03/07	38.9	38.3
3	80 (-1)	MII (1)	1:100 (-1)	H (1)	1/26/08	38.9	23.6
4	40 (1)	MII (1)	1:100 (-1)	L (-1)	1/23/08	3.6	4.1
5	80 (-1)	FUM (-1)	1:10 (1)	H (1)	10/31/07	40.4	5.6
6	40 (1)	FUM (-1)	1:10 (1)	L (-1)	10/30/07	4.5	5.9
7	80 (-1)	MII (1)	1:10 (1)	L (-1)	9/27/07	3.1	3.6
8	40 (1)	MII (1)	1:10 (1)	H (1)	10/18/07	38.9	26.1

5.9.2 DoE Predictive Model Results

The results of this seven (7) Degree of Freedom (DoF) analysis were used to develop an equation which shows the cell parameter inter-relationships between ESA, MEM, CONC, and TEMP.

$$E1 = 13.825 + 4.775*ESA + 0.525*MEM - 3.525*CONC + 9.575*TEMP - 4.025*ESA*MEM + 0.925*ESA*CONC + 4.025*ESA*TEMP \quad \textit{Equation 8}$$

Inspection of Equation 8 shows that cell temperature is the most important independent factor affecting cell output voltage and the interaction between ESA and CONC the least important. In order to obtain Standard Error (SE) and 95% CI data, the lowest contributing 2-way interaction effect was removed and a 6 DoF analysis re-run with the resulting predictive equation presented in Equation 9.

$$E1\ (SE)\ [\pm CI] = 13.825 + 4.775*ESA + 0.525*MEM - 3.525*CONC + 9.575*TEMP - 4.025*ESA*MEM + 4.025*ESA*TEMP \quad \textit{Equation 9}$$

In equation 8, the values of ESA are either -1 (low, 80 mesh) or +1 (high, 40 mesh); values of MEM are either (low, Fumasep®) or +1 (high, MII); values of CONC are either -1 (low, 1:100) or +1 (high, 1:10); and values of TEMP are either -1 (low, 5 °C) or +1 (high, 40 °C). With 80 mesh electrodes, MII membrane, 1:10 Concentration, and Room Temperature (RT), Equation 9 predicts:

E1 = 13.825 + 4.775*(-1) + 0.525*(+1) – 3.525*(+1) + 9.575*(0) – 4.025*(-1)*(+1) + 4.025*(-1)*(0) = 10.1 mV (2.068) [-16.2, 36.36].

This compares favorably to the actual measured result of 15.5 mV for this condition. Additional related 6 DoF SAS DoE analysis information is presented in the following 6 figures, Figures 5.42 to 5.47 which comprise the full report.

ADX Report for 500 Ohm Loaded Concentration Cell - Full Recycle

Today's date:	01AUG2008
Experiment creation date:	01AUG2008

Design Details

Design Details

Design Type	Two-level
Design Description	1/2 Fraction
Number of factors	4
Number of runs	8
Resolution	4

Factors and Responses

Factor	Low	Center	High	Response
ESA	-1	0	1	E1
MEM	-1	0	1	
CONC	-1	0	1	
TEMP	-1	0	1	

Confounding Rules

TEMP = ESA*MEM*CONC

Alias Structure (up to 2FI)

ESA*MEM + CONC*TEMP
ESA*CONC + MEM*TEMP
ESA*TEMP + MEM*CONC

Design Points

Coded Design

Figure 5.42 SAS 6 DoF Input Model Data (1 of 6)

ADX Report for 500 Ohm Loaded Concentration Cell - Full Recycle

RUN	ESA	MEM	CONC	TEMP	E1
1	-1	-1	-1	-1	3.4
2	1	-1	-1	1	38.3
3	-1	1	-1	1	23.6
4	1	1	-1	-1	4.1
5	-1	-1	1	1	5.6
6	1	-1	1	-1	5.9
7	-1	1	1	-1	3.6
8	1	1	1	1	26.1

Uncoded Design

RUN	ESA	MEM	CONC	TEMP	E1
1	-1	-1	-1	-1	3.4
2	1	-1	-1	1	38.3
3	-1	1	-1	1	23.6
4	1	1	-1	-1	4.1
5	-1	-1	1	1	5.6
6	1	-1	1	-1	5.9
7	-1	1	1	-1	3.6
8	1	1	1	1	26.1

Explore

Main effects plot for E1

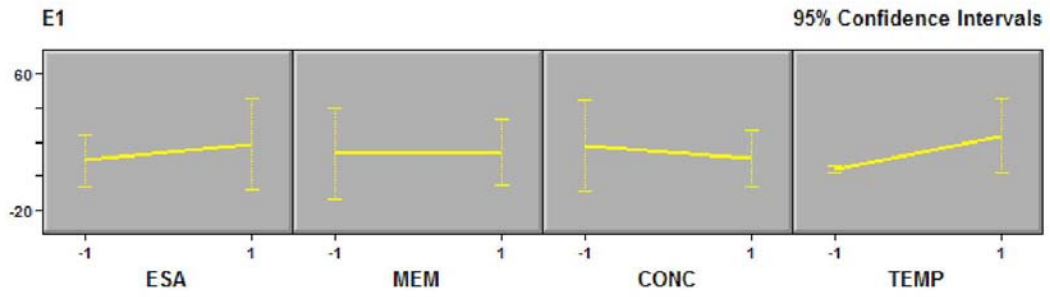

Interaction plot for E1

Figure 5.43 SAS 6 DoF Input Model Data (2 of 6)

	Master Model	Predictive Model
RMSE	.	2.616295
R-square	100.0%	99.47%
Adjusted R-square	.	96.27%
Coefficient of Variation	.	18.92438

Alias Structure for E1

Master Model	Predictive Model
ESA*MEM + CONC*TEMP	No effects aliased.
ESA*CONC + MEM*TEMP	
ESA*TEMP + MEM*CONC	

Predictive Model for E1

Coded Levels(-1,1)	
E1 =	13.825 + 4.775*ESA + 0.525*MEM - 3.525*CONC + 9.575*TEMP
	- 4.025*ESA*MEM + 4.025*ESA*TEMP
Uncoded Levels	
E1 =	13.825 + 4.775*ESA + 0.525*MEM - 3.525*CONC + 9.575*TEMP
	- 4.025*ESA*MEM + 4.025*ESA*TEMP

Effects for E1

	Master Model				Predictive Model			
Term	Estimate	Std Err	t	Pr > |t|	Estimate	Std Err	t	Pr > |t|
ESA	9.55	.	.	0.0001	9.55	1.85	5.162162	0.121815
MEM	1.05	.	.	0.0001	1.05	1.85	0.567568	0.671357
CONC	-7.05	.	.	0.0001	-7.05	1.85	-3.81081	0.163373
TEMP	19.15	.	.	0.0001	19.15	1.85	10.35135	0.061311
ESA*MEM	-8.05	.	.	0.0001				
ESA*CONC	1.85	.	.	0.0001				
ESA*TEMP	8.05	.	.	0.0001				

Effect estimates for E1

Figure 5.44 SAS 6 DoF Predicted Model Results (3 of 6)

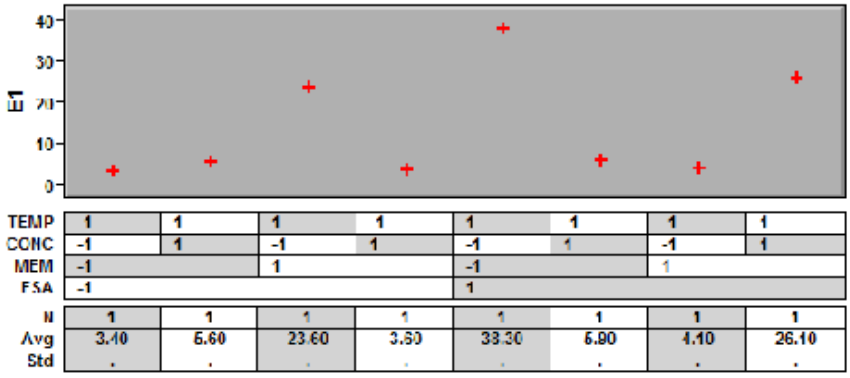

Fit Details

Fit for E1

ANOVA for E1

	Master Model					Predictive Model				
Source	DF	SS	MS	F	Pr > F	DF	SS	MS	F	Pr > F
ESA	1	182.405	182.405	.	0.0001	1	182.405	182.405	26.64792	0.121815
MEM	1	2.205	2.205	.	0.0001	1	2.205	2.205	0.322133	0.671357
CONC	1	99.405	99.405	.	0.0001	1	99.405	99.405	14.52228	0.163373
TEMP	1	733.445	733.445	.	0.0001	1	733.445	733.445	107.1505	0.061311
ESA*MEM	0	0	.	.	0.0001	1	129.605	129.605	18.93426	0.143807
ESA*CONC	0	0	.	.	0.0001					
ESA*TEMP	0	0	.	.	0.0001	1	129.605	129.605	18.93426	0.143807
MEM*CONC	0	0	.	.	0.0001					
MEM*TEMP	0	0	.	.	0.0001					
CONC*TEMP	0	0	.	.	0.0001					
Model	7	1283.515	183.3593	.	0.0001	6	1276.67	212.7783	31.08522	0.13644
Error	0	4.22E-13	.			1	6.845	6.845		
Total	7	1283.515				7	1283.515			

Fit Statistics for E1

Figure 5.45 SAS 6 DoF Predicted Model Results (4 of 6)

Effect	Estimate	Std Error	t Ratio	P Value
ESA	9.55	.	.	.
MEM	1.05	.	.	.
CONC	-7.05	.	.	.
TEMP	19.15	.	.	.
ESA*MEM + ...	-8.05	.	.	.
ESA*CONC + ...	1.85	.	.	.
ESA*TEMP + ...	8.05	.	.	.

Pareto plot for E1

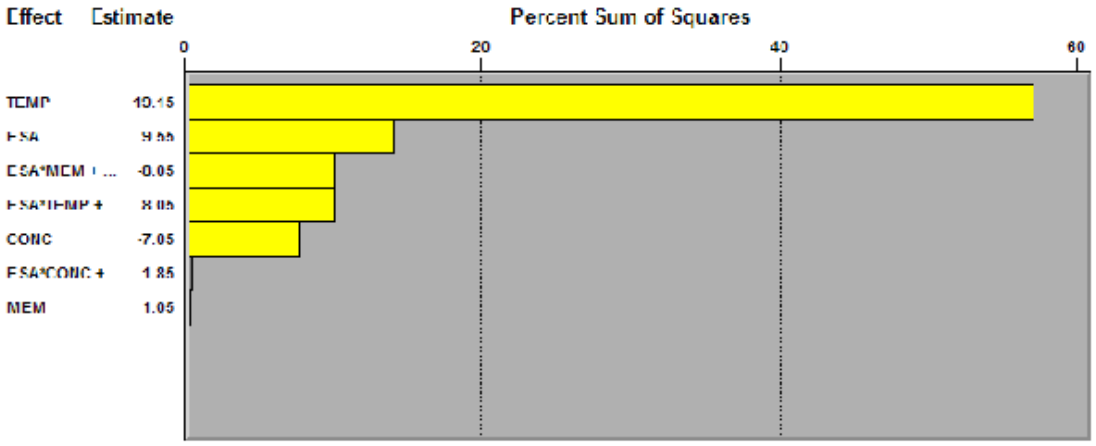

Normal plot for E1

Figure 5.46 SAS 6 DoF Predicted Model Results (5 of 6)

ADX Report for 500 Ohm Loaded Concentration Cell - Full Recycle

E1				
D(E1)	=	0 when E1	<	0
D(E1)	=	0.5 when E1	=	12.5
D(E1)	=	1 when E1	>	25
Power	=	1 for lower half		
Power	=	1 for upper half		

Prediction Profile Settings

Factor	Optimal Setting
ESA	0
MEM	0
CONC	0
TEMP	0

Response	Estimated Value
E1	13.825 [2.071761,25.57824]
Desirability	55.30%

Response Calculator

ESA	MEM	CONC	TEMP	E1
-1	-1	-1	-1	2.475 (2.447)[-28.6,33.57]
1	-1	-1	1	39.23 (2.447)[8.129,70.32]
-1	1	-1	1	22.68 (2.447)[-8.42,53.77]
1	1	-1	-1	5.025 (2.447)[-26.1,36.12]
-1	-1	1	1	6.525 (2.447)[-24.6,37.62]
1	-1	1	-1	4.975 (2.447)[-26.1,36.07]
-1	1	1	-1	4.525 (2.447)[-26.6,35.62]
1	1	1	1	25.18 (2.447)[-5.92,56.27]
-1	1	1	0	10.08 (2.068)[-16.2,36.36]
-1	1	1	1	15.63 (2.447)[-15.5,46.72]
-1	1	-1	-1	11.58 (2.447)[-19.5,42.67]
-1	1	-1	0	17.13 (2.068)[-9.16,43.41]
0	0	0	0	13.83 (0.925)[2.072,25.58]
1	-1	1	1	32.18 (2.447)[1.079,63.27]
-1	1	0	0	13.6 (1.85)[-9.91,37.11]
1	1	1	0	11.58 (2.068)[-14.7,37.86]
-1	1	1	0	10.08 (2.068)[-16.2,36.36]
1	1	-1	0	18.63 (2.068)[-7.66,44.91]
-1	1	-1	0	17.13 (2.068)[-9.16,43.41]

Prediction profile plot

Figure 5.47 SAS 6 DoF Predicted Model Results (6 of 6)

5.9.3 Measured Test Data vs. Predicted 6 DoF Model Results

Examination of the DoE main effects plot for E1 reveal that the membrane end use type, manufacture, and physical characteristics made very little difference in the cell output performance. Temperature was the major parameter evaluated, as indicated in both the E1 main effects and Pareto plots.

Additional data analysis and testing was performed, using the easier to use MII membrane, to quantify the model skill vs. actual loaded measured cell performance vice operational temperature and solution concentration gradient. Modeled data input values were computed using Equation 6, and are displayed in Table 5.4 along with the corresponding measured cell data. All data is presented in Figure 5.48 along with the standard error and 95% CI bars.

Table 5.4 Measured Test Data vs. Predicted 6 DoF Model Results

Run	ESA	MEM	CONC	Temp °C	Type	Date	Cell Voltage (mV DC)
1	80 (-1)	MII (1)	1:10 (1)	3.95	Model	8/1/08	4.5
2	80 (-1)	MII (1)	1:10 (1)	21.63	Model	8/1/08	10.1
3	80 (-1)	MII (1)	1:10 (1)	39.3	Model	8/1/08	15.6
4	80 (-1)	MII (1)	1:10 (1)	3.1	Measured	9/27/07	3.6
5	80 (-1)	MII (1)	1:10 (1)	21.8	Measured	2/22/08	15.4
6	80 (-1)	MII (1)	1:10 (1)	36.8	Measured	2/23/08	24.6
7	80 (-1)	MII (1)	1:100 (-1)	3.95	Model	8/1/08	11.6
8	80 (-1)	MII (1)	1:100 (-1)	21.63	Model	8/1/08	17.1
9	80 (-1)	MII (1)	1:100 (-1)	39.3	Model	8/1/08	22.7
10	80 (-1)	MII (1)	1:100 (-1)	3	Measured	1/31/08	8.4
11	80 (-1)	MII (1)	1:100 (-1)	22.3	Measured	2/15/08	15.4
12	80 (-1)	MII (1)	1:100 (-1)	38.9	Measured	1/26/08	23.6

Analysis of Figure 5.48 reveals that a ten-fold increase in cell temperature (4 to 40 °C) for an 80 Mesh electrode resulted in a:

1) Two fold increase in membrane potential (Δ = 11.1 mV) with a 1:100 concentration difference, slightly less than predicted by Nernst (Δ = 14.3 mV),
2) Four (4) fold increase in membrane potential (Δ = 11.1 mV) with a 1:10 concentration difference, slightly more than predicted by Nernst (Δ = 7.5 mV).

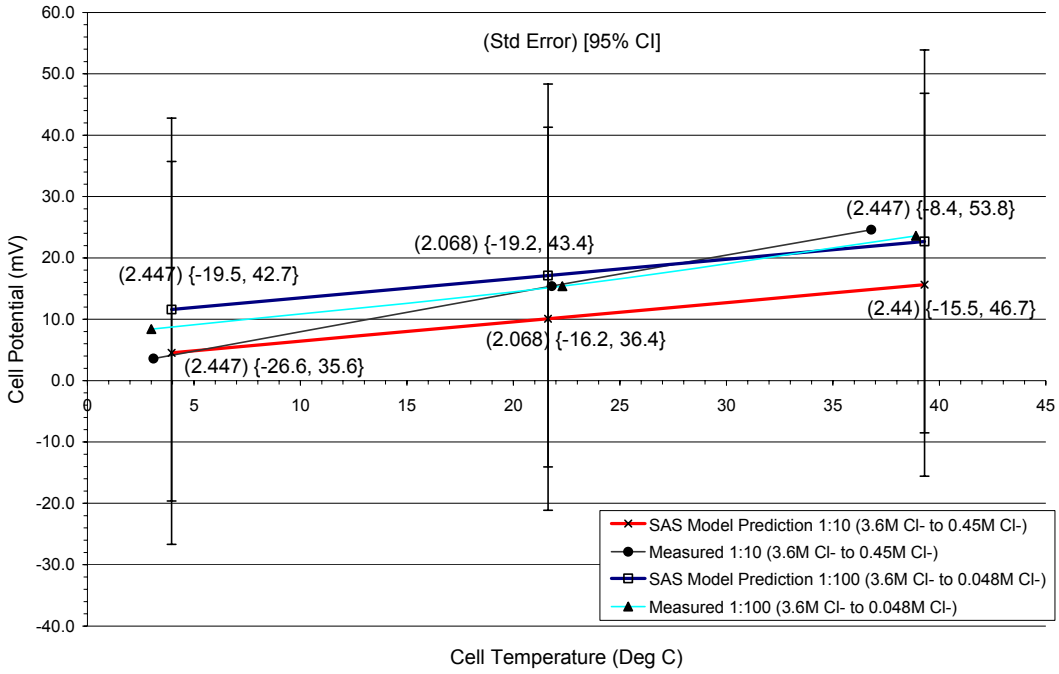

Figure 5.48 Measured Test Data vs. Predicted 6 DoF Model Results

The predicted loaded cell membrane potential is fairly linear with a consistent offset between 1:10 and 1:100 concentration differences. Measured results indicate that although generally matching the predicted values, the magnitude of the variation is less and then only at the min/max temperatures – no difference was noted with concentration variations at room temperature with the MII membrane. All measured values under load are significantly lower than the OCV values predicted by via the Nernst equation.

Equation 9 predicts a 15% increase in E1 for a 40 mesh electrode over an 80 mesh electrode at a 1:10 concentration ratio and similarly a 9% increase at a 1:100 concentration ratio. Recalling that the 40 mesh electrode should have 11% more surface

area than the 80 mesh electrode, this provides an indication of the DoE model skill while confirming both that an increase in surface area results in a better charge collector and the near-linear relation with concentration ratio.

5.10 Micro Electrical Mechanical Systems Suitability Discussion

A comparison of energy sources for nano and micro systems and energy harvesting applications is presented in Figure 5.49.

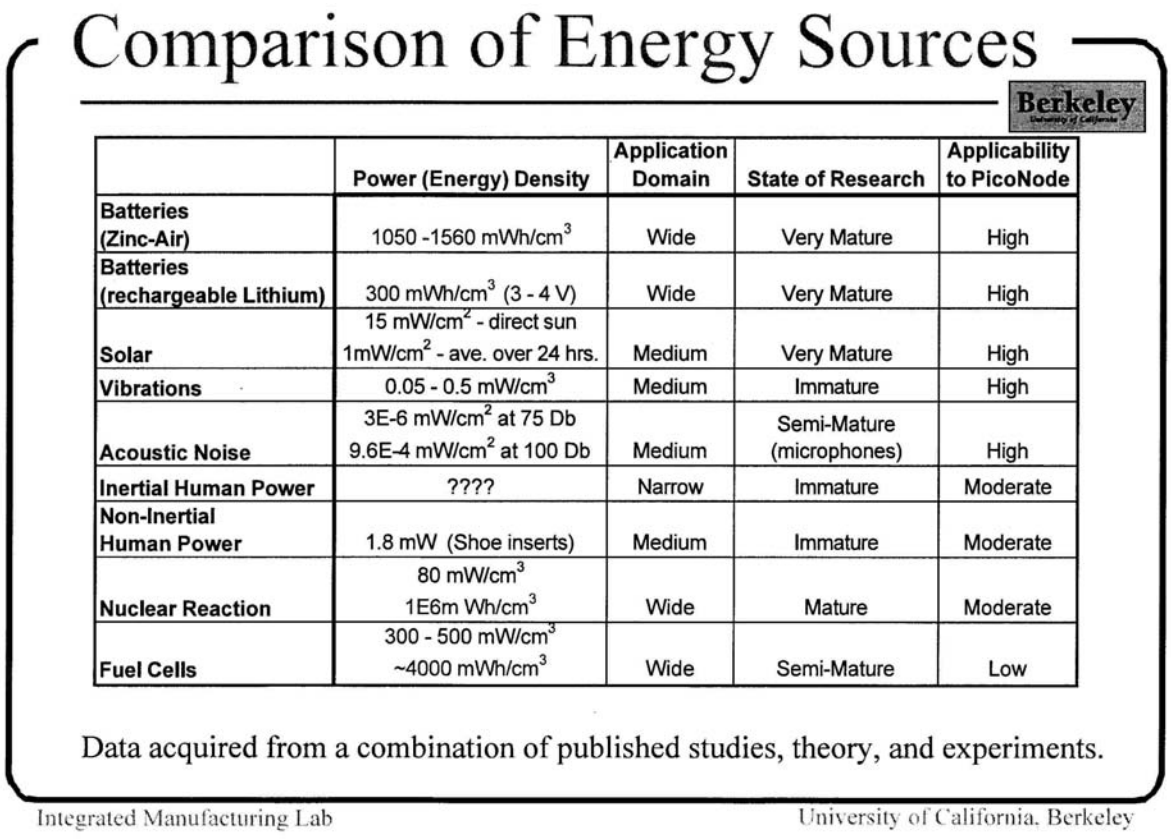

	Power (Energy) Density	Application Domain	State of Research	Applicability to PicoNode
Batteries (Zinc-Air)	1050 -1560 mWh/cm^3	Wide	Very Mature	High
Batteries (rechargeable Lithium)	300 mWh/cm^3 (3 - 4 V)	Wide	Very Mature	High
Solar	15 mW/cm^2 - direct sun 1mW/cm^2 - ave. over 24 hrs.	Medium	Very Mature	High
Vibrations	0.05 - 0.5 mW/cm^3	Medium	Immature	High
Acoustic Noise	3E-6 mW/cm^2 at 75 Db 9.6E-4 mW/cm^2 at 100 Db	Medium	Semi-Mature (microphones)	High
Inertial Human Power	????	Narrow	Immature	Moderate
Non-Inertial Human Power	1.8 mW (Shoe inserts)	Medium	Immature	Moderate
Nuclear Reaction	80 mW/cm^3 1E6m Wh/cm^3	Wide	Mature	Moderate
Fuel Cells	300 - 500 mW/cm^3 ~4000 mWh/cm^3	Wide	Semi-Mature	Low

Figure 5.49 Comparisons of Energy Sources for Energy Harvesting Applications

Table 5.3 measured cell output test result average resulted in:

1) Average Measured Instantaneous Current = 2.77E-05 Amps
   (0.028 milli Amps or 28 micro Amps),
2) Average Measured Instantaneous Voltage = 0.0138 Volts (13.8 mVolts) ,
3) Average Measured Instantaneous Power = 3.8E-7 Watts
   (0.38 micro Watts or 382 pico Watts).

In Comparisons from Figure 5.49:

1) Meso-scale low cost Pico Radio limits power dissipation from picoWatts/cm2 to 100microWatt/cm2 for energy scavenging target,
2) MEMS-device operations falls between picoWatts/cm2 to Watts/cm2,
3) Standard solar cells produce 15 milliWatt/cm2 in bright sun, 1 milliWatt/cm2 when averaged over 24 hours, 6 microWatt/cm2 inside a typically illuminated office,
4) Methanol Micro-Fuel Cell operational targets to match Li-ion polymer in cell phone applications are between 150 - 200 milliWatt/cm2,
5) Traditional PEM based fuel cells are between 300 - 500 milliWatt/cm3.

In Summary: All though the industry trend is toward lower power devices, 382 picoWatts is Orders of Magnitude below target PEM or Methanol Micro-Fuel Cell or Li-ion polymer cell phone batteries. It is, however, in the low range of nano/MEMS or Energy Harvesting Devices.

Chapter 6

Summary and Future Research

The focus of this Ph.D. research effort was to address the concept, research and evaluation of a Bi-Polar membrane based seawater concentration cell and its sutability as a low power energy source for Energy Harvesting nano/MEMS devices.

In support of this, increased technical understanding into the membrane, ionic, environmental, and electrochemical effects on the generated membrane current and potential of a Bi-Polar membrane based, seawater concentration cell was developed. This was done thru: the use of equivalent circuit modeling to establish membrane, electrode processes and kinetics; an evaluation of pertinent factors effecting cell output performance followed by screening experiments to reduce the number of factors to a manageable quantity for testing; and a Design of Experiment based fractional factorial design analyses with accompanying performance testing to determine a predictive cell output performance optimized model in terms of pertinent input parameters tested. Modeled performance output was then compared to actual test measurements with nominal output values compared against other types of energy sources for nano and micro systems and energy harvesting application. The final results confirmed that the

average cell output value of 380 picoWatts falls within the power range required for MEMS or Energy Harvesting Devices.

Contributions to the field included the development of an increased technical understanding into a novel fuel cell based design method and apparatus which uses a replenishing concentration differential of ion solutions across a Bi-Polar semi-permeable membrane to effect ion mobility and electrical power generation. The feasibility and applicability of this Bi-Polar membrane based Dialytic Power Generator was in turn evaulated as a power source for low power systems such as energy harvesting devices, where it is impossible or impractable to provide wired or traditional battery power.

During the testing process, the following specific contributions were identified:

1) Confirmed the Ag wire mesh electrode functioned simply as charge collectors and the material selection, design, and ruggedness is suitable for subsequent field testing,

2) Identified membrane swelling and linkage of the "openings" present in used CEM and AEM membranes that can account for the measured Cl^- co-ion/counter-ion migration across the Bi-Polar membrane from the concentrated to dilute sides of the functioning Bi-Polar concentration cell,

3) Determined that for maximum potential output, the cell needs to operated in what is typically referred to as the (+) Bi-Polar membrane orientation, that being with the

concentrated solution in contact with the Bi-Polar membrane AEM side and the Bi-Polar membrane CEM in contact with the dilute solution side,

4) Determined that Anomalous Positive Osmosis and co-ion/counter-ion migration effects are occurring simultaneously across the Bi-Polar membrane,

5) Determined an insensitivity in cell output performance due to changes in fluid pumping speed across the flow rates tested,

6) Determined that although OCV variations occurred with cell agitation, the affects were small under load with equilibrium quickly reached once agitation is removed,

7) Determined that Bi-Polar membrane concentration cell operation under external loading can not be described adequately by the Nernst equation,

8) Determined that membrane end use type/manufacture made very little difference and that temperature was the primary driving factor in terms of the cell output potential,

9) The Bi-Polar membrane seawater concentration cell under an external electrical load produced a near constant current output across the load conditions tested,

10) The Bi-Polar membrane seawater concentration cell under an external electrical load operates as an electrolytic capacitor when operated in a fuel cell configuration,

In general, although small in output power, when under external load, the cell was found to produce repeatable results while relatively invariant to concentration variations and overall motion. All good characteristics for a Dialytic based sea water concentration cell power generator.

Significant progress was made during this research effort. Additional research is planned to continue this progess to futher develop the concept into a functioning energy generation system. This research would entail investigating output performance changes through: changes in cell design and size scalability; differing configuration combinations; and alternate electrode selection. In addition, the possible existance of Bi-Polar Membrane "water splitting" effects will be examined.

Bibliography

1. Maron, S.H. and Prutton, C.F., "Principals of Physical Chemistry", The Macmillan Company, New York, 1962 (fourth printing) – LOC: 58-5133, pp. 544-569.

2. Bard, A.J. and Faulkner, L.R., "Electrochemical Methods – Fundementals and Applications", Wiley and Sons, 20001, Second edition.

3. Kemperman, A. J. B., "Handbook on Bi-Polar Membrane Technology", Twente University Press, The Netherlands, 2000.

4. Higa, M. and Kira, A, "Transport of Ions across Bi-Polar membranes. 1. Theoretical and Experimental Examination of the Membrane Potential of KCL Solutions", J. Phys. Chem., Vol. 99, 1995, pp. 5089 - 5093.

5. Scott, Keith, "Handbook of Industrial Membranes", 1995, Elsevier Advanced Technology, Oxford, ISBN 1856172333.

6. Helfferich, F., "Ion Exchange", 1962, McGraw-Hill, New York.

7. Mulder, M., "Basic Principles of Membrane Technology, second edition", Kluwer Academic Publishers, 2003.

8. Mattson, M.E. and Lew, M., Desalination, Vol. 41, 1982, page 1.

9. Solt, G. in "Handbook of Water Purification", Lorch, W., ed. McGraw-Hill, London, 1981, Chapter 9.

10. Pretz, J., Staude, E., "Reverse Electrodialysis (RED) with Bi-Polar Membranes, an Energy Storage System", Berichte der Bunsenges. Phys. Chem., Vol. 102, No. 4, 1998, pp. 676-685.

11. Applegate, L. E., "Membrane Separation Processes", J. of Chemical Engineering, June 11, 1984, pp. 64-89.

12. Libes, S., "An Introduction to Marine Biogeochemistry", John Wiley & Sons, 1992, ISBN 0471509469.

13. Kudela, V., Richau, K., Bleha, M., Paul, D., "Orientation effects on Bi-Polar and other asymmetric membranes as observed by concentration potentials", Separation and Purification Technology, Vol. 22-23, 2001, pp. 655-662.

14. Suendo, V., Eto, R., Osaki, T., Higa, M., Tanioka, A., "Ionic Environmental Effect on the Time-Dependent Characteristics of Membrane Potential in a Bi-Polar membrane", Journal of Colloid and Interface Science, Vol. 240, 2001, pp. 162-171.

15. Strathmann, H., Krol, J.J., Rapp, H. J., and Eigenberger, G., Journal of Membrane Science, Vol. 125, 1997, pp. 125.

16. Strathmann, H., Bauer, B., Rapp, H., "Better Bi-Polar membranes", Chemtech, June 1993, pp. 17 – 24.

17. Rubinstein, I., Warshawsky, A., Schechtman, L., Kedem, O., Desalination, Vol. 55, 1984, pp. 55.

18. Simons, R., "The origin and elimination of water splitting in ion exchange membranes during water demineralization by electrodialysis", Desalination, Vol. 28, 1979, pp. 41-42.

19. Mani, K.N., "Electrodialysis water splitting technology", Journal of Membrane Science, Vol. 58, 1991, pp 117-138.

20. Vlahakis, J., Jacobsen, W., and Miller, G., Electrotechnology, Vol. 1, Ann Arbor, Michigan, 1978, pp. 15.

21. Wang, H., Yu, Z., Wang, E., "The Transfer of Chloride Ion Across an Anion Exchange Membrane", Electroanalysis, Vol. 8, No. 8-9, 1996, pp. 821-825.

22. Ohya, H., "Dialytic Battery Convertible Free Energy of Mixing of Seawater and River Water", The 3rd Pacific Chemical Engineering Congress, Seoul, Korea, May 8-11, 1983, pp 451-456, Proceedings.

23. Cyclic Voltammetry Primer, www-biol.paisley.ac.uk/marco/enzyme_electrode/chapter1/cyclic_voltammetry1.htm.

24. Uhlig, H., "Uhlig's Corrosion Handbook", John Wiley & Sons, 2000, Second edition.

25. EIS Primer - Application Note, "Basics of Electrochemical Impedance Spectroscopy", Gamry Instruments, Warminster, Pa, 2007.

26. Gabrielli, Claude, "Use and Application of Electrochemical Impedance Techniques", Technical Report Number 24, Solartron Analytical, April 1997.

27. Bockris, J., Drazic, D., "Electro-Chemical Science", Taylor and Francis, Ltd, 1972.

About the Author

Clifford Ronald Merz is currently the Director and Program Engineer for the University of South Florida (USF)/College of Marine Science's Coastal Ocean Monitoring and Prediction System (COMPS) Program. He holds a bachelor degree in Ocean Engineering from Florida Atlantic University (1984) and is a licensed Professional Engineer in the State of Florida. In 2003, he formed Dialytics, Inc., a technology start up company specializing in renewable energy and water reuse concepts. He is married to his wife Michelle of 26 years and has five beautiful children: Zachary, Rachel, Melissa, Eric, and Trent.

After obtaining his BS degree, he went back to school part-time to refine his professional skills, leading to advanced MS degrees in Ocean (1986), Civil/Water Resources Engineering (1997), and a graduate certificate in Desalination Technology and Engineering (2003). Most recently completing hands-on field installation workshops in solar, wind, and biodiesel through the Midwest Renewable Energy Association.